Updates to the MAX IV 1.5 GeV Storage Ring Lattice

Simon C. Leemann

March 13, 2012 (updated June 11, 2012)

MAX-lab Internal Note 20120313[1]

Abstract

As a result of detailed magnet [1] and vacuum [2] design work, the lattice for the MAX IV 1.5 GeV storage ring has been modified. The lattice files have been updated: a new 20120313 branch [3] will replace the previous 20111102 branch. The updated lattice uses the same slice model as the previous branch (albeit with minor modifications to the focusing gradients in order to restore the desired tune and straight section optics), but sextupole positions and strengths have changed slightly. Therefore, nonlinear optics have been re-optimized. This note summarizes the changes in the new lattice branch and attempts to investigate performance and error-tolerance of the new linear and nonlinear optics. In this sense it can be considered an update of the DDR chapter on beam dynamics in the 1.5 GeV storage ring [4]. The note concludes with a list of current lattice files and their purpose.

1 Summary of Changes in the New Lattice

The following is a summary of changes applied to the 20111102 branch resulting in the new 20120313 branch.

- The dimension of the injection septum has been updated to match recent specifications [5]. The magnetic length of the device is 1021 mm. Note however, that the injection point (i.e. the magnetic end of the septum) is left unchanged, i.e. it is still 1252 mm downstream of the center of the injection straight.

[1] This document is available for download at `http://www.maxlab.lu.se/node/999`

- The magnetic length of SCi has increased from 20 mm to 55 mm while the magnetic length of SCo has increased from 20 mm to 50 mm. These magnets have also been shifted away from the adjacent SQFi/o.
- The BPM at the center of the achromat has been move out of the SCi structure.
- The length of the BPM's has been reduced from 50 mm to 30 mm. The BPM's were moved by 20 mm into the straights and away from SQFi by 32.5 mm, respectively.
- The horizontal pinger PH (magnetic length 300 mm), which is identical to the dipole injection kicker KI, has been installed in straight no. 1. It is in the same location as KI in straight no. 3: its center is 548 mm downstream of the girder end marker (GE).
- The vertical pinger PV (magnetic length 150 mm) was moved within straight no. 1. Its center is 918 mm downstream of the girder end marker (GE).
- The dipole injection kicker KI is not explicitly mentioned in the lattice. Its center is at the location of the center of the PSM which is installed in the lattice file.
- The nomenclature in the lattice file has been updated.
- The linear and nonlinear optics have been updated (see below).

2 Updated Linear Optics

The magnet slice model for the 1.5 GeV storage ring was retained from the previous lattice branch. The actual bending angles and gradients were however updated according to the detailed magnet design in [1]. In order to restore the design optics and working points, several scalings were applied:

- The dipole field and gradients in DIP were scaled simulating a change of current to the dipole in order to achieve the design bending angle of 15°: $f_{\mathrm{deg}} = 0.99930346$.
- The straight section optics and working point were restored by scaling the gradients in the dipoles and quadrupoles: $f_{\mathrm{DIP}} = 0.99987651$, $f_{\mathrm{SQFi}} = 0.96939705$, $f_{\mathrm{SQFo}} = 0.98444233$. In the real machine the former corresponds to an excitation of the pole-face strips (PFS's) while the latter can be accomplished by changing the currents to the quadrupoles.

The original optics were restored very well with these adjustments. The sole exception is a minor increase in horizontal beta function: $\beta_x = 5.672\,\mathrm{m} \rightarrow 5.684\,\mathrm{m}$. An overview if the optics and lattice properties are given in Fig. 1 and Table 1.

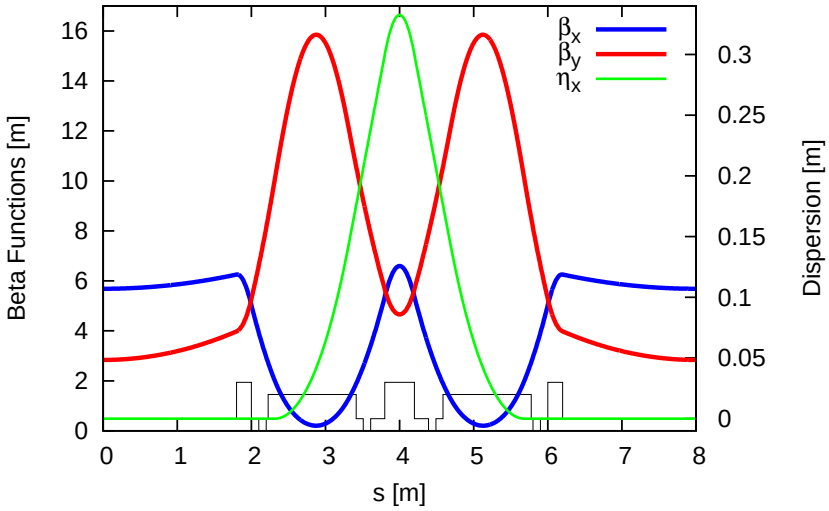

Figure 1: The updated optics in one of the 12 DBA's of the MAX IV 1.5 GeV storage ring. The magnetic structure is indicated at the bottom.

Table 1: The most important properties of the updated lattice for the MAX IV 1.5 GeV storage ring.

Periodicity	12
Circumference	96 m
Horizontal tune ν_x	11.22
Vertical tune ν_y	3.15
Natural horizontal chromaticity ξ_x	-22.964
Natural vertical chromaticity ξ_y	-17.154
Momentum compaction (linear) α_c	3.055×10^{-3}
Horizontal damping partition J_x	1.464
Bare lattice emittance ε_0	5.982 nm rad
Bare lattice energy loss per turn	114.1 keV
Bare lattice natural energy spread σ_δ	0.745×10^{-3}
Bare lattice horizontal damping time τ_x	5.751 ms
Bare lattice vertical damping time τ_y	8.417 ms
Bare lattice longitudinal damping time τ_E	5.479 ms

3 Updated Nonlinear Optics

With the updated linear and nonlinear optics the natural chromaticity has slightly shifted: $\xi_x = -22.933 \rightarrow -22.964$ and $\xi_y = -17.149 \rightarrow -17.145$. In order to correct this linear chromaticity to +2.0 in both planes the sextupole component of SQFi is adjusted by scaling with $f_{\mathrm{SQFi},2} = 0.997853$ and setting $(b_3)_{\mathrm{SDi}} = -74.067033\,\mathrm{m}^{-3}$. In addition, the nonlinear dynamics are improved by the following harmonic sextupole settings: the sextupole component of SQFo is left unscaled, i.e. $f_{\mathrm{SQFo},2} = 1.00$ and SDo is set to $(b_3)_{\mathrm{SDo}} = -101.92\,\mathrm{m}^{-3}$. This constitutes the 521 nonlinear optics. The tune footprint and dynamic aperture (DA) for the m5-20120313-521 lattice are displayed in Figs. 2 and 3. The large apparent vertical DA available for low horizontal amplitudes is an artifact: an island structure was not recognized by the adaptive step control causing the island to be considered to be part of the continuous DA. The available off-momentum DA for ±4% is required to achieve the target lattice momentum acceptance (MA).

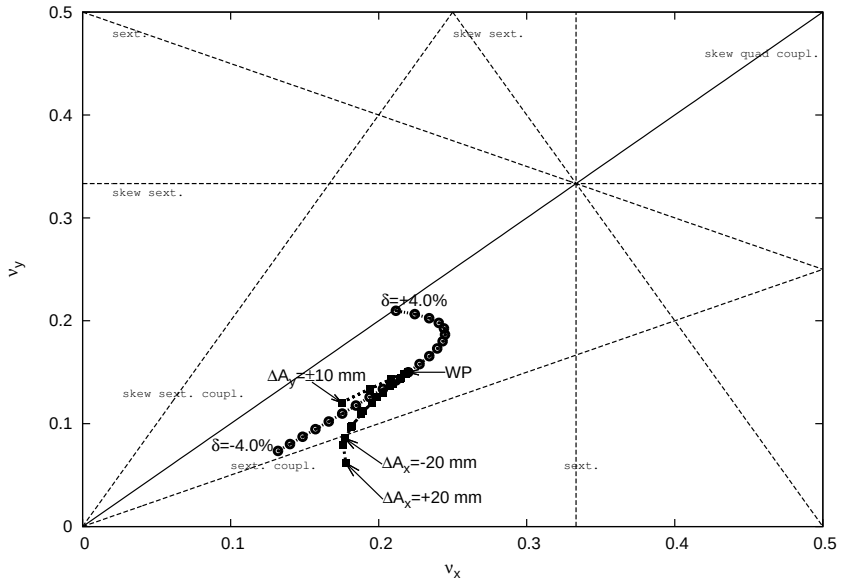

Figure 2: The tune footprint of the new m5-20120313-521 optics of the MAX IV 1.5 GeV storage ring.

Several diffusion and frequency maps have been generated for the new m5-20120313-521 optics. Figs. 4 and 5 show tune diffusion for on and off-momentum particles. The on-momentum diffusion map (DM) was limited so as to exclude the island above the continuous DA. The on-momentum frequency map analysis (FMA)

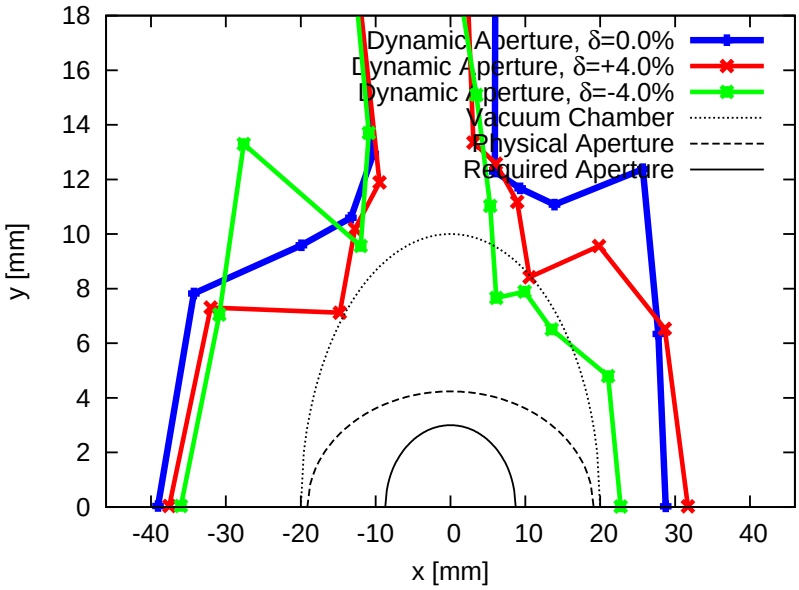

Figure 3: Dynamic aperture calculated with Tracy-3 in 6D for the new m5-20120313-521 optics of the MAX IV 1.5 GeV storage ring.

reveals that the area required for injection and lifetime show low diffusion. The increased diffusion observed in the semicircular strip around $(-23/+20, 0) \times (0, 10)$ is caused by $6\nu_x = 67$ while the semicircular strip around $(-20/+16, 0) \times (0, 12)$ is caused by $\nu_x - 2\nu_y = 5$. The lower part of the on-momentum frequency map (FM) appears to show "folded" diffusion, but this is just an artifact of diffusion of particles that have crossed the integer resonance $\nu_y = 3$ (this happens only for very large horizontal amplitudes).

The off-momentum DM reveals increased diffusion around $\delta = -5\%$ caused by crossing the sextupole coupling resonance $\nu_x - 2\nu_y = 5$. The resonance $6\nu_x = 67$ leads to increased diffusion around $\delta = -2.75\%$, whereas $6\nu_y = 19$ leads to increased diffusion around $\delta = +1\%$. Slightly elevated levels of diffusion are caused by $\nu_x + 4\nu_y = 24$ which is encountered for $\delta = 2.75\%$. The coupling resonance $\nu_x - \nu_y = 8$ is crossed around $\delta = 4\%$, but this is not resolved by the DM presented here. Finally, slightly elevated levels of diffusion are caused by $\nu_x + 4\nu_y = 24$ which is encountered once more at $\delta = 5.75\%$.

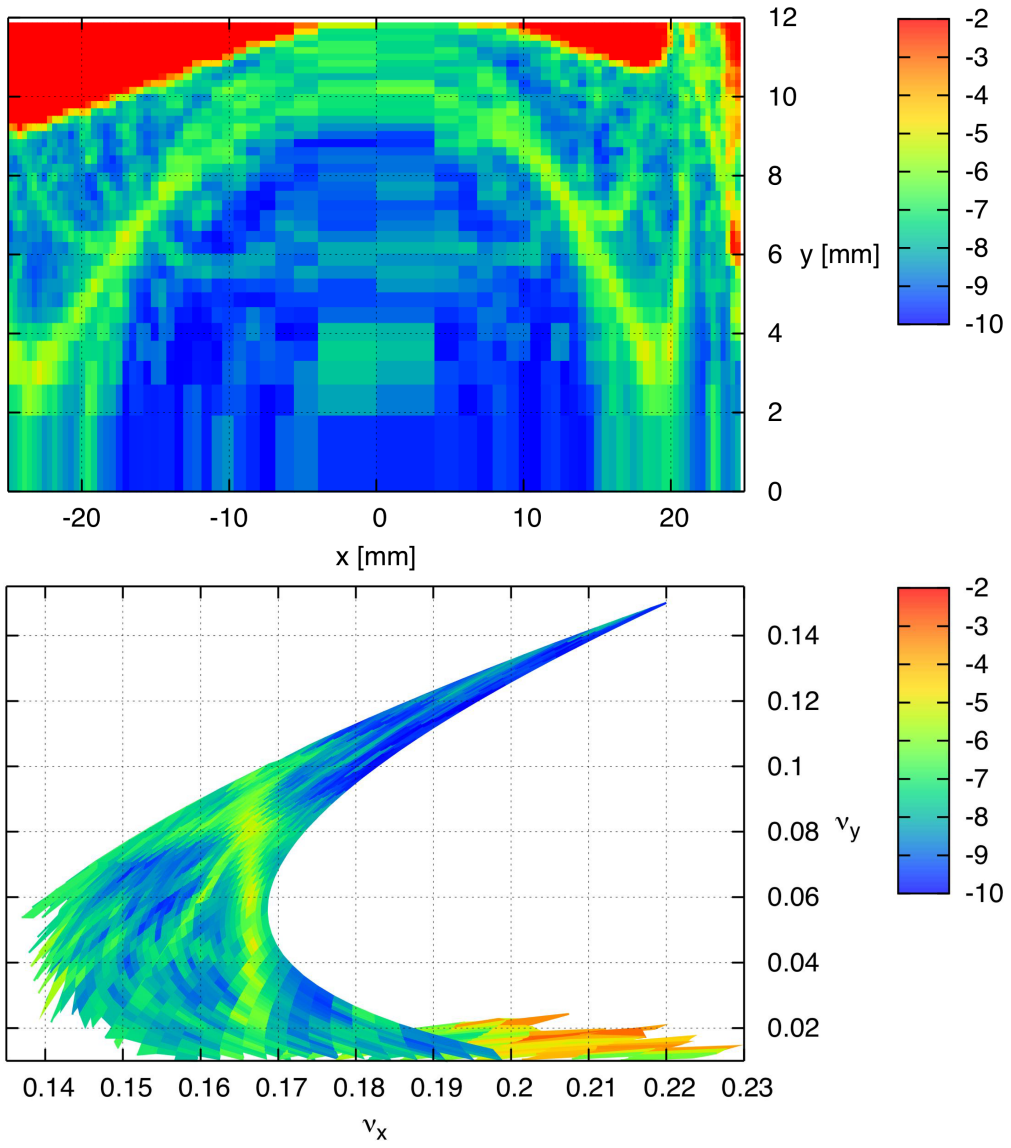

Figure 4: Frequency map analysis with Tracy-3 for the new m5-20120313-521 optics of the MAX IV 1.5 GeV storage ring. Top: Diffusion map for on-momentum particles. Bottom: Frequency map corresponding to data points plotted in top plot.

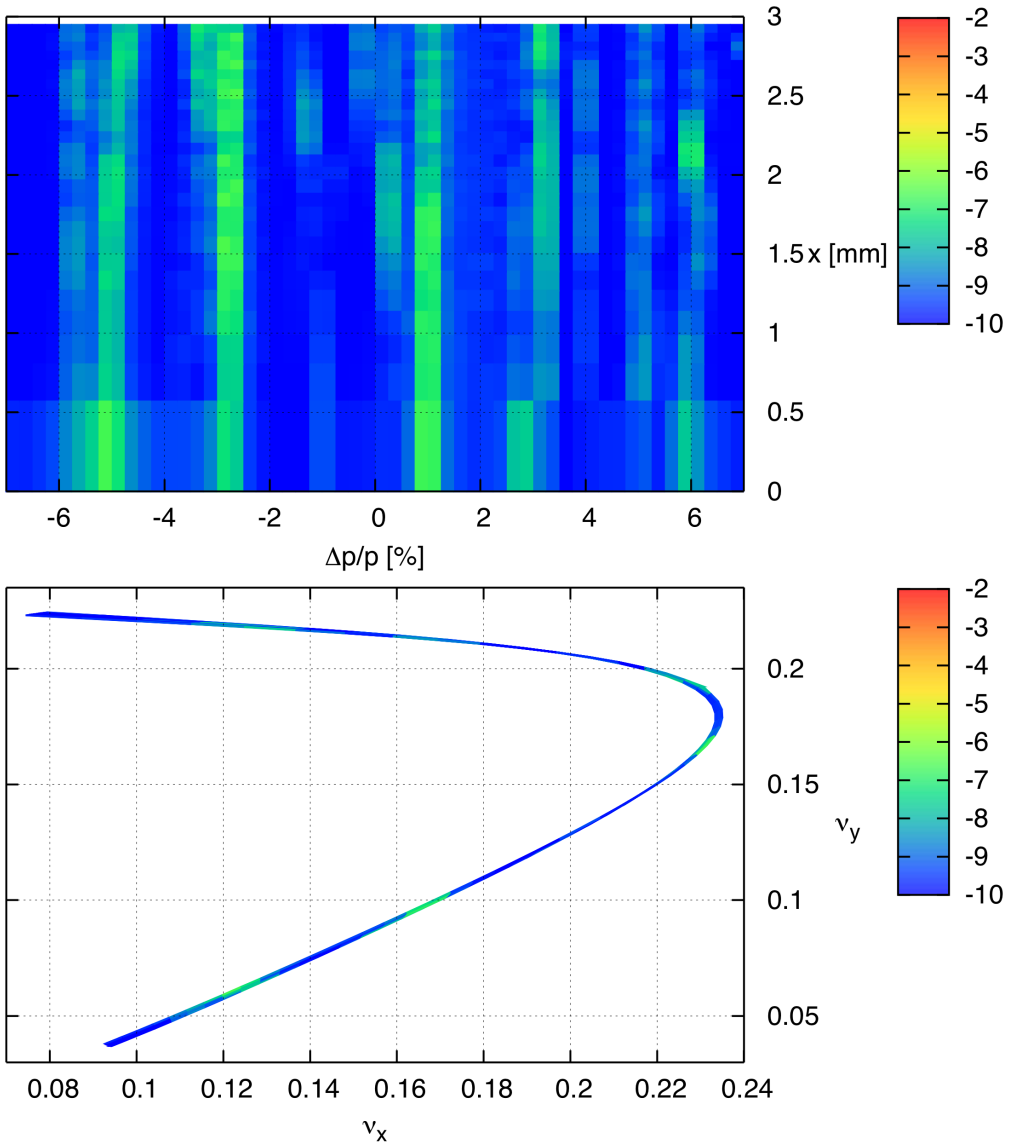

Figure 5: Frequency map analysis with Tracy-3 for the new m5-20120313-521 optics of the MAX IV 1.5 GeV storage ring. Top: Diffusion map for on-momentum particles. Bottom: Frequency map corresponding to data points plotted in top plot (upper lobe corresponds to positive momentum offsets).

In the MAX IV 1.5 GeV storage ring the chromaticity correction and nonlinear optics are achieved by the built-in sextupole components in the SQFi/o magnets as well as the dedicated SDi/o. An alternative nonlinear optics setting attempts to correct the linear chromaticity to +1.0 in both planes. This is achieved by powering the correction sextupoles SCi and changing the current setting on the SDi. In addition, the correction sextupole SCo and SDo settings are varied as well to improve the nonlinear dynamics. The resulting optics is referred to as m5-20120313-523.

Table 2: List of sextupole gradient changes by magnet family required to correct the linear chromaticity to +1.0 in both planes.

Magnet family	Sextupole gradient change	Rel. difference
SDi	$b_3 = -74.067033\,\mathrm{m}^{-3} \longrightarrow -68.325710\,\mathrm{m}^{-3}$	−7.8%
SDo	$b_3 = -101.920\,\mathrm{m}^{-3} \longrightarrow -99.520\,\mathrm{m}^{-3}$	−2.4%
SCi	$b_3 = 0.000\,\mathrm{m}^{-3} \longrightarrow -8.556585\,\mathrm{m}^{-3}$	n/a
SCo	$b_3 = 0.000\,\mathrm{m}^{-3} \longrightarrow -9.600\,\mathrm{m}^{-3}$	n/a

The tune footprint and dynamic aperture (DA) for the m5-20120313-523 lattice are displayed in Figs. 6 and 7. Compared to the 521 nonlinear optics, the 523 nonlinear optics show a much more compressed tune footprint both for large amplitudes and momentum offsets. Since the chromatic tune shifts are wrapped up more tightly in the 523 nonlinear optics, the distance to the linear coupling resonance for large positive momentum deviations is increased. This is reflected by the DA: while the on-momentum DA is comparable, the DA at $\delta = \pm 4.0\%$ for 523 is increased so it almost matches the on-momentum DA.

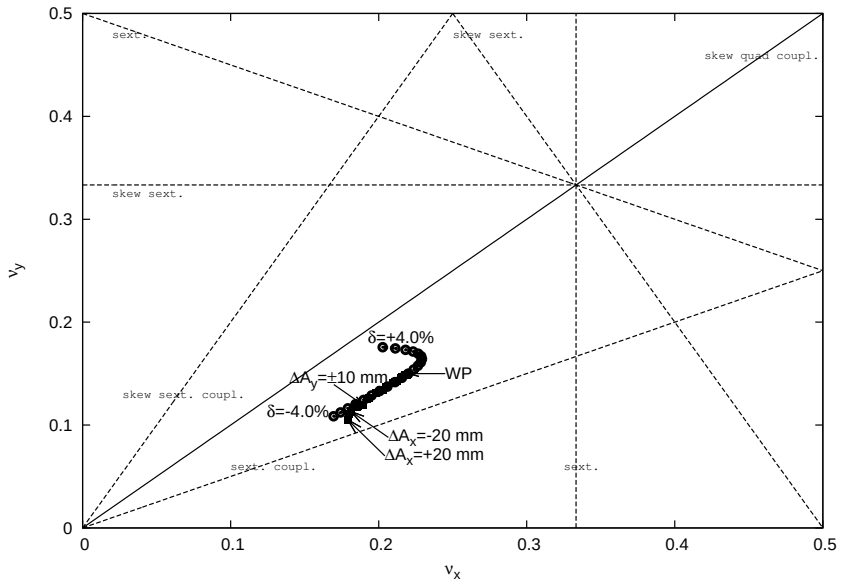

Figure 6: The tune footprint of the new m5-20120313-523 optics of the MAX IV 1.5 GeV storage ring.

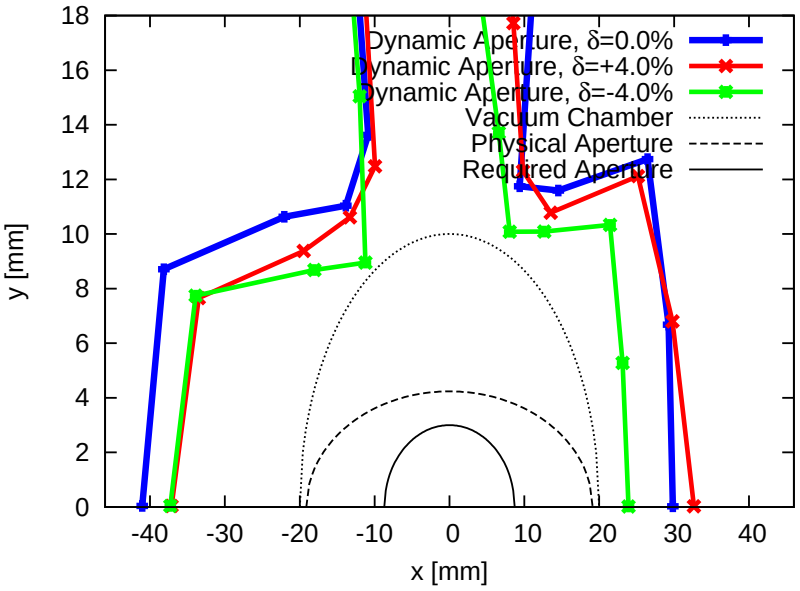

Figure 7: Dynamic aperture calculated with Tracy-3 in 6D for the new m5-20120313-523 optics of the MAX IV 1.5 GeV storage ring.

Frequency map analysis has also been performed for the new m5-20120313-523 optics. Figs. 8 and 9 show tune diffusion for on and off-momentum particles. The on-momentum diffusion map (DM) was again limited so as to exclude the island above the continuous DA. The on-momentum FMA reveals again that the area required for injection and lifetime show low diffusion. The increased diffusion observed in the semicircular strip around $(+23/-27, 0) \times (0, 11)$ is caused by $\nu_x - 2\nu_y = 5$. Slightly elevated diffusion occurs in the vicinity of $(0, 3.5)$. This is caused by crossing $4\nu_x + \nu_y = 48$.

The off-momentum DM reveals increased diffusion around $\delta = -5.25\%$ caused by crossing $6\nu_x = 67$. Slightly elevated diffusion occurs in the vicinity of $\delta = -0.75\%$. This is caused by crossing $4\nu_x + \nu_y = 48$. Increased levels of diffusion encountered around $\delta = 2.5\%$ are the result of crossing $6\nu_y = 19$. The coupling resonance $\nu_x - \nu_y = 8$ is crossed just slightly above $\delta = 4.5\%$, but this is not resolved by the DM presented here. The crossing of $6\nu_x = 67$ then causes elevated diffusion around $\delta = 5\%$ as does crossing $2\nu_x + 4\nu_y = 35$ around $\delta = 6.25\%$.

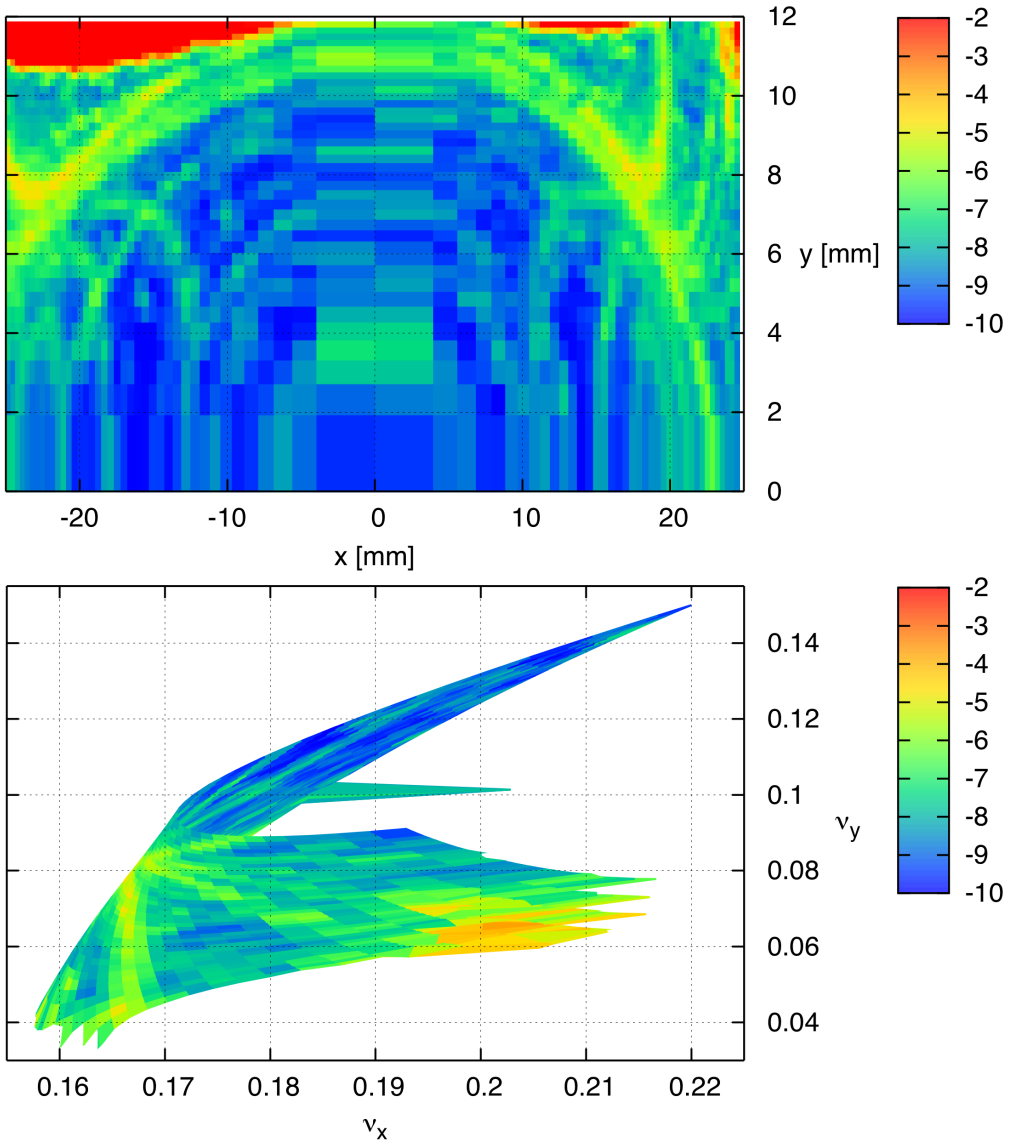

Figure 8: Frequency map analysis with Tracy-3 for the new m5-20120313-523 optics of the MAX IV 1.5 GeV storage ring. Top: Diffusion map for on-momentum particles. Bottom: Frequency map corresponding to data points plotted in top plot.

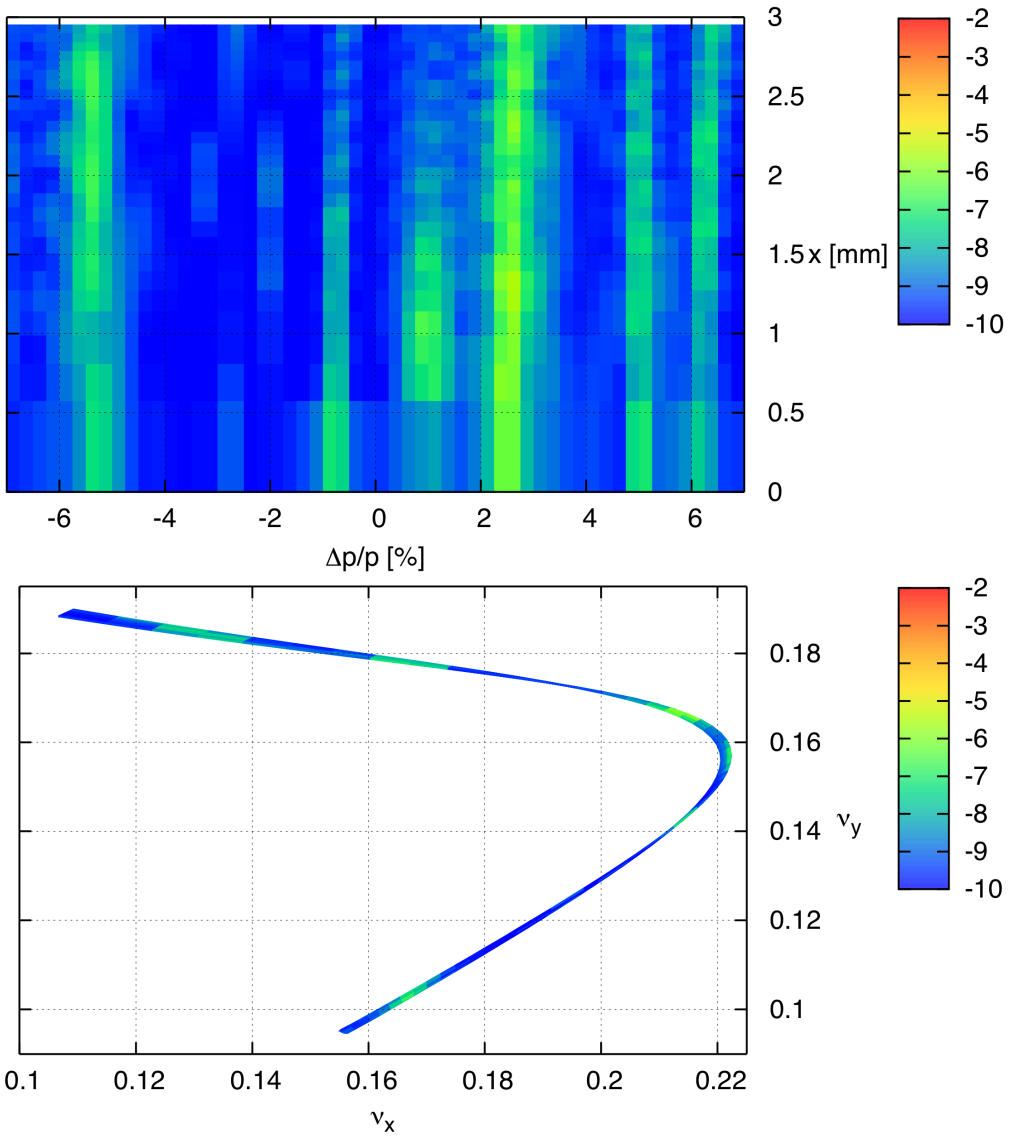

Figure 9: Frequency map analysis with Tracy-3 for the new m5-20120313-523 optics of the MAX IV 1.5 GeV storage ring. Top: Diffusion map for on-momentum particles. Bottom: Frequency map corresponding to data points plotted in top plot (upper lobe corresponds to positive momentum offsets).

4 Expected Performance of the New Lattice

This section attempts to give performance estimates for the new lattice in a realistic environment, e.g. a situation where the lattice is subjected to alignment errors and has magnets with field and multipole errors. For the studies presented in this section, the lattice m5-20120313-523-bare has been used since this is the optics foreseen for user operation. The first part deals with errors and their effect on DA of the new lattice. The section after then discusses intrabeam scattering (IBS), emittance, and expected Touschek lifetime.

4.1 A Realistic Machine – the New Lattice with Errors

In this section errors are applied to the bare lattice and the expected DA of such a machine is presented and discussed. The error models used are similar to those used in the DDR.

4.1.1 Alignment Errors

A first study concerns the effect of alignment errors on dynamic aperture. The error model makes the following assumptions:

- Magnet blocks are misaligned in the horizontal and vertical by 50 μm rms. The rms roll error is 0.2 mrad. This is modeled as Gaussian distribution with a 2σ cut-off. Survey and alignment experts expect less than 100 μm displacement of neighboring blocks.
- Dipoles, quadrupoles, sextupoles, and dipole corrector magnets are misaligned individually within each magnet block by 25 μm rms in the horizontal and vertical. Their individual roll errors are 0.2 mrad rms. This is an attempt at modeling the machining accuracy. The model again assumes a Gaussian distribution with a 2σ cut-off.
- BPM calibration errors are assumed to be 3 μm rms in both planes together with a 0.1 mrad rms roll error.

Figures 10 (before correction) and 11 (after correction) show the closed-orbit deviations in each achromat for 100 turns in a machine that has been misaligned using this error model. The orbit correction makes use of the 36 BPM's and 72 dipole correctors in the bare lattice. However, this model is somewhat unphysical and as a consequence pessimistic. Since the BPM's are included as part of the "girder" in the lattice file, they are misaligned from the "design" orbit systematically together with the other elements within the same magnet block. As a consequence this leads to

apparently large rms closed-orbit variations after correction ($\approx 35\,\mu$m at the center of the straights in both planes, i.e. on the same order as the misalignments). In the real machine however, this "design" orbit does not exist. Instead, the magnet centers define an "ideal" orbit to which the BPM's are calibrated and to which, later, ID's are aligned. Therefore, despite the rigid fixture of the BPM's to the magnets within the magnet block and the resulting misalignment as a consequence of the block misalignment, BPM calibration results in orbit correction to the "ideal" orbit with much smaller deviations than indicated by Fig. 11 where the deviations to the artificial "design" orbit have been plotted.

The required corrector strengths are displayed in Fig. 12. It is evident that the required rms strengths stay well below $100\,\mu$rad for all corrector locations. The DA of a bare lattice with misalignments after orbit correction is displayed in Fig. 13. The DA is clipped in the vertical plane because of the previously mentioned island. The achieved on-momentum DA (after orbit correction) for all seeds is beyond the vacuum chamber, i.e. definitely sufficient.

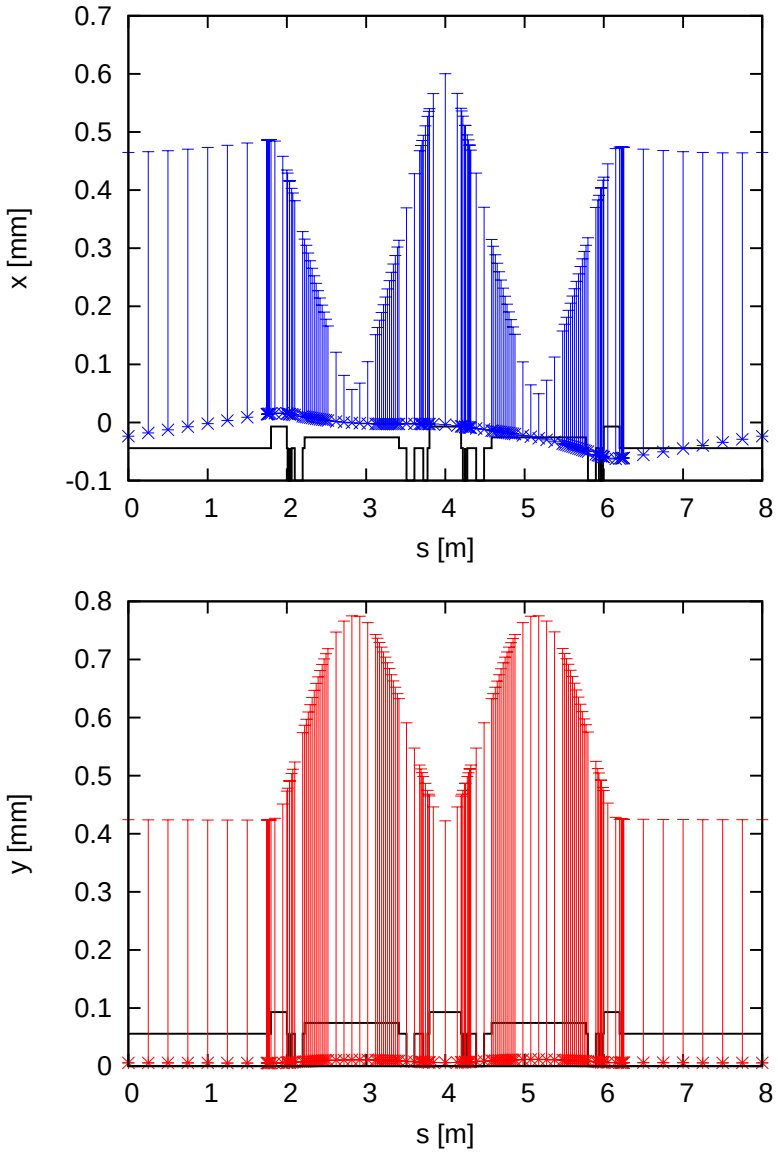

Figure 10: Closed-orbit deviations from the design orbit after applying misalignments but without correcting the orbit. 100 misaligned machine seeds were used. The dot shows the mean deviation for all seeds and the "error bar" depicts the deviation corresponding to 1 standard deviation across all seeds.

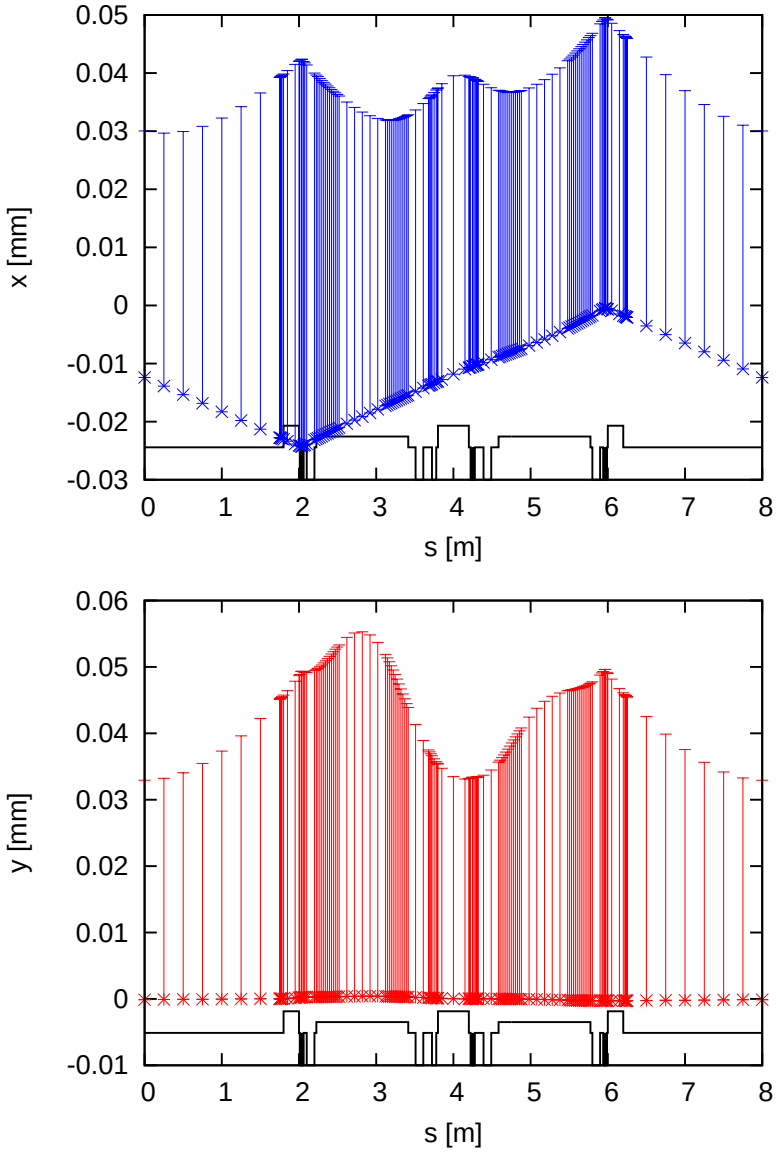

Figure 11: Closed-orbit deviations from the design orbit after applying misalignments and after applying orbit correction with 72 dipole correctors. 100 misaligned machine seeds were used. The dot shows the mean deviation for all seeds and the "error bar" depicts the deviation corresponding to 1 standard deviation across all seeds.

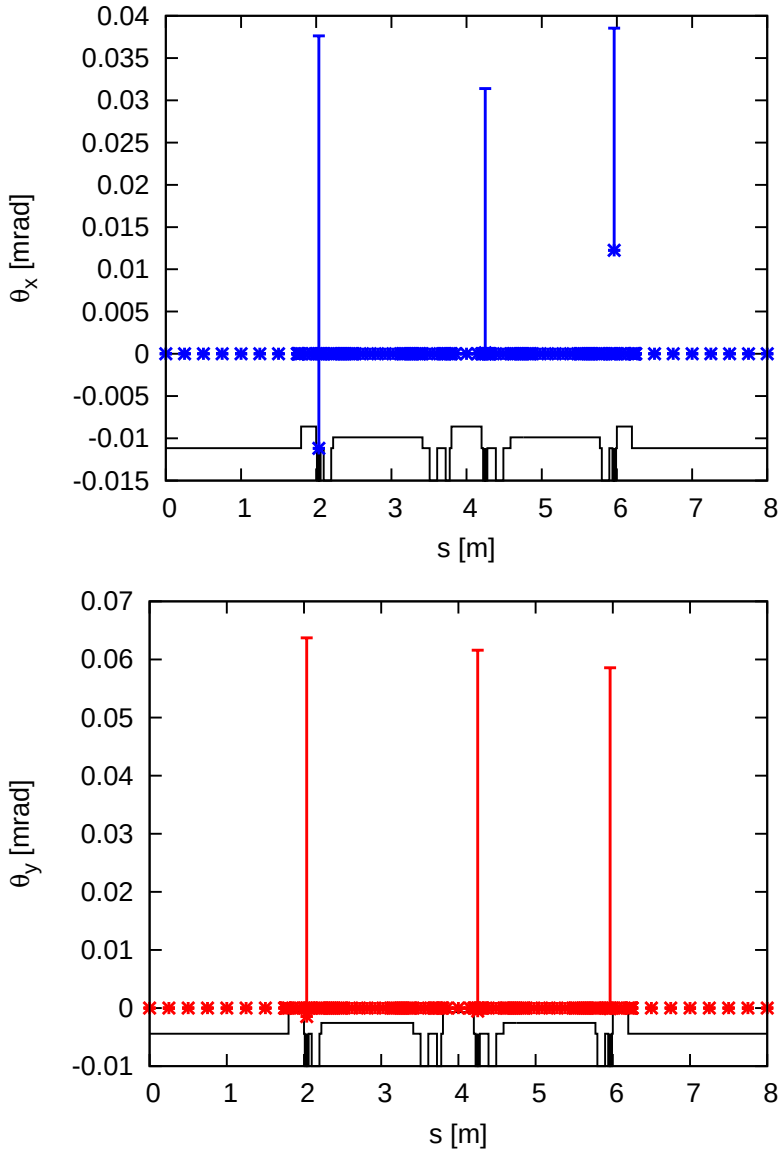

Figure 12: Corrector strengths required for the orbit correction displayed in Fig. 11. 100 misaligned machine seeds were used. The dot shows the mean corrector strength for all seeds and the "error bar" depicts the deviation corresponding to 1 standard deviation across all seeds.

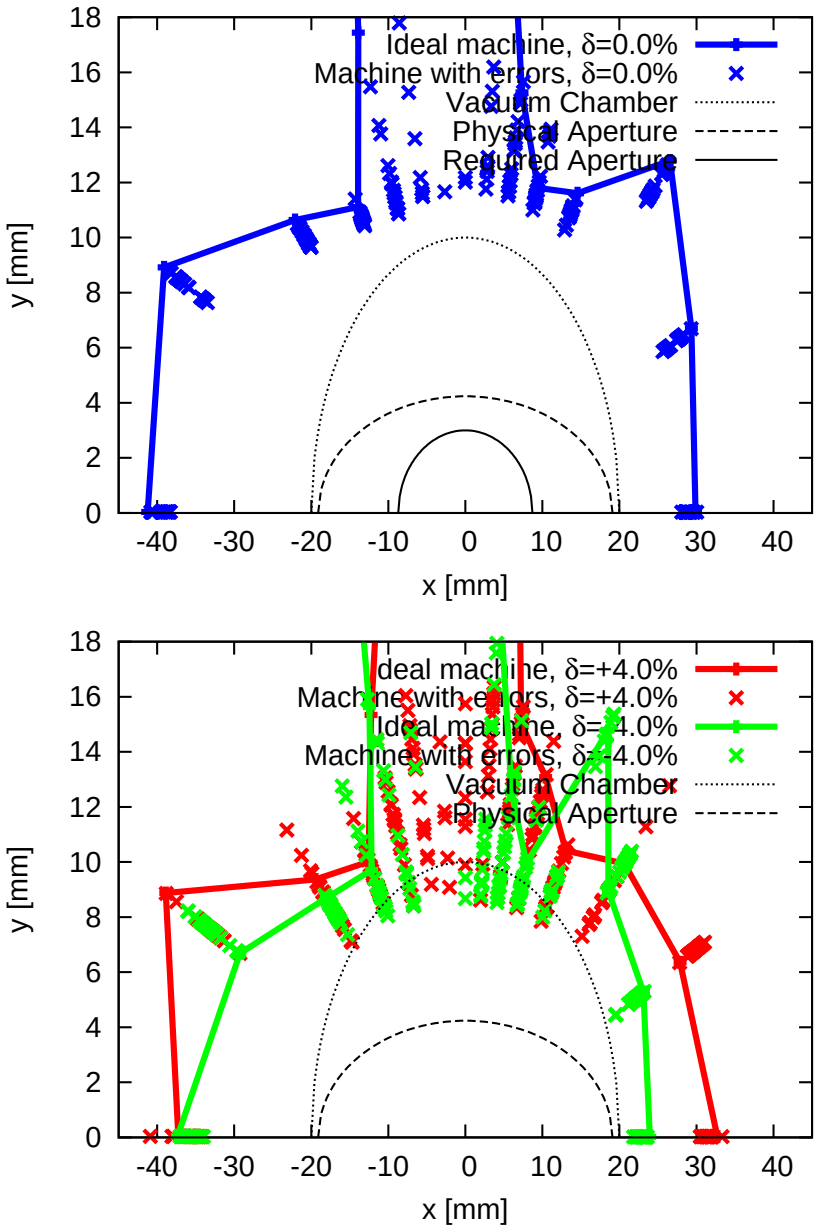

Figure 13: Dynamic aperture at the center of the straight section in the MAX IV 1.5 GeV storage ring (bare lattice) from tracking with Tracy-3. The plots show the ideal lattice (solid line) and results for 20 seeds with misalignments (crosses). Top: On-energy DA. Bottom: Off-energy DA.

4.1.2 Field and Multipole Errors

The next step is to assess the DA of a bare lattice when an error model for magnet field and multipole errors is included. The multipole error model is identical to the one used in the DDR (cf. Table 3.7). The field errors in the magnets were modeled by applying a random 0.2% rms error to the gradients in the dipoles and quadrupoles as well as a random 0.2% rms error to the sextupole gradients. These errors were applied as Gaussian distributions with a 2σ cut-off. The resulting DA is displayed in Fig. 14. A very substantial reduction of DA is recognized.

Figure 15 shows the same DA, but this time using only gradient errors in the dipoles and quadrupoles. Clearly, the DA reduction observed above has its source in gradient errors in the dipoles and quadrupoles, but not in the sextupoles or from the multipole errors. In fact, by inspecting the DA resulting from gradient errors in the dipoles alone (cf. Fig. 16) it can be determined that this is actually the main source of the DA reduction observed in Fig. 14.

The DA reduction caused by the gradient variation in the dipoles is unacceptably severe. Fortunately, these variations can be reduced by shunting dipoles to gradients (and consequently using orbit correctors to correct the variation of bending angles) or by using individual power supplies to power the pole-face strips (PFS's) on each dipole. If such a procedure is followed, the gradient errors in the dipoles can be substantially reduced. For the studies presented here, the underlying assumption is that gradient errors can be reduced to a level of 0.02% rms (Gaussian, 2σ cut-off). Results for a DA where the standard multipole error model along with the 0.02% rms variation of all gradients has been applied are shown in Fig. 17. Clearly this leads to DA which is comparable to the DA as a result of misalignments and again perfectly acceptable since it extends beyond the vacuum chamber.

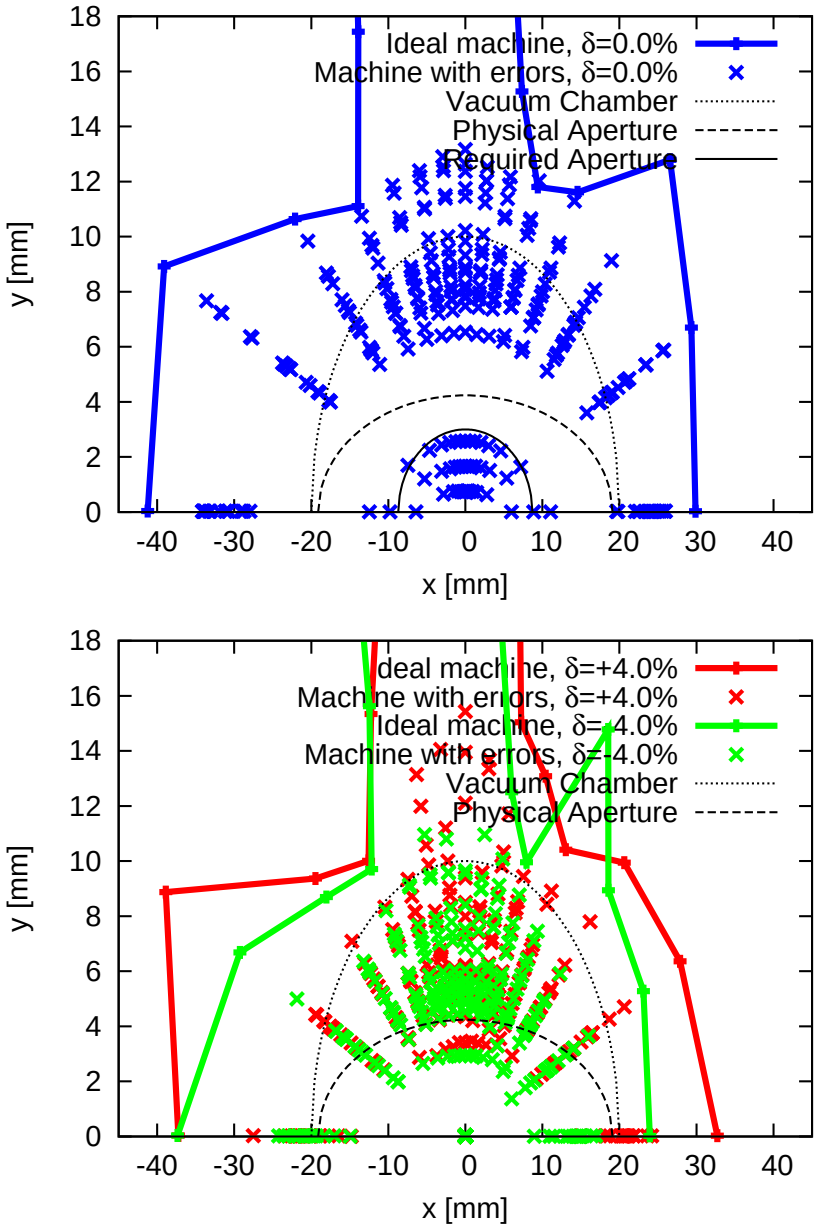

Figure 14: Dynamic aperture at the center of the straight section in the MAX IV 1.5 GeV storage ring (bare lattice) from tracking with Tracy-3. The plots show the ideal lattice (solid line) and results for 20 seeds with field and multipole errors (crosses). For the field errors a 0.2% rms variation of all gradients in the dipoles and quadrupoles as well as a 0.2% rms variation of all sextupole gradients was assumed. Top: On-energy DA. Bottom: Off-energy DA.

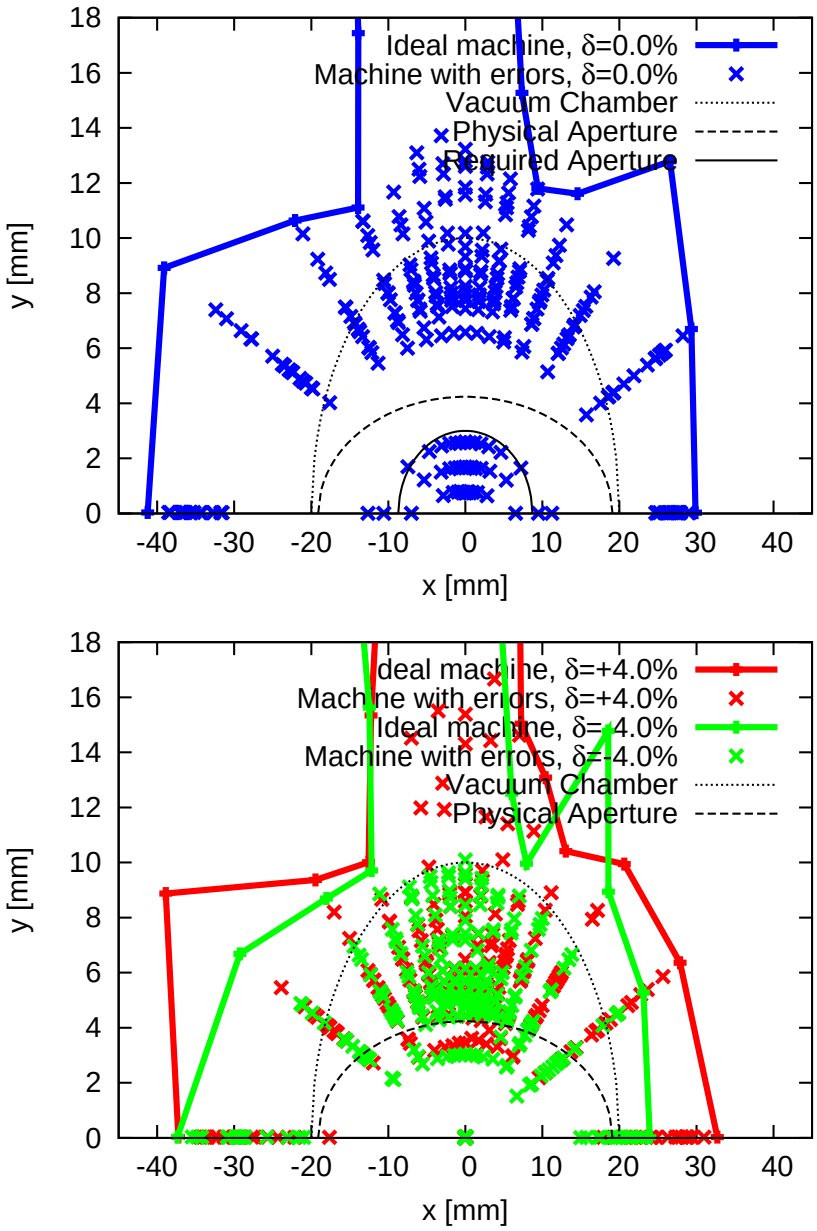

Figure 15: Dynamic aperture at the center of the straight section in the MAX IV 1.5 GeV storage ring (bare lattice) from tracking with Tracy-3. The plots show the ideal lattice (solid line) and results for 20 seeds with field and multipole errors (crosses). For the field errors a 0.2% rms variation of all gradients in the dipoles and quadrupoles was assumed. Top: On-energy DA. Bottom: Off-energy DA.

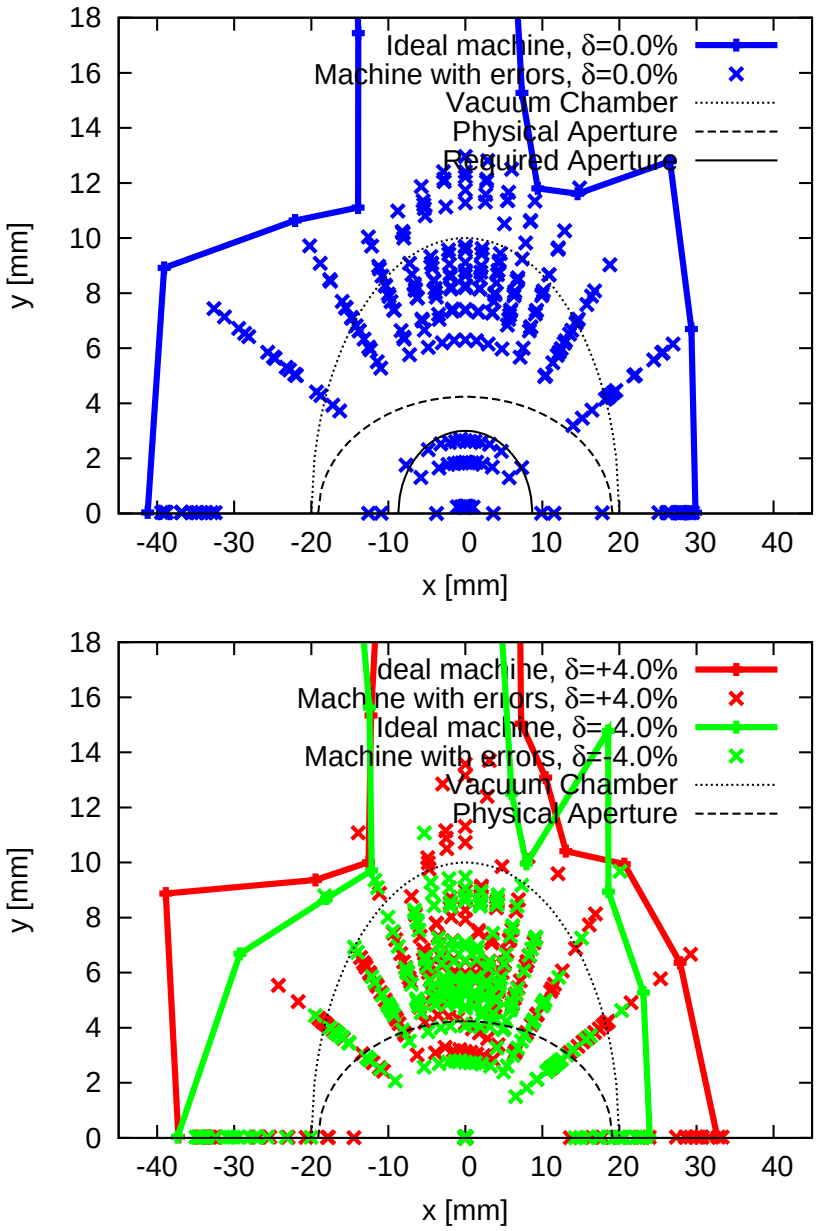

Figure 16: Dynamic aperture at the center of the straight section in the MAX IV 1.5 GeV storage ring (bare lattice) from tracking with Tracy-3. The plots show the ideal lattice (solid line) and results for 20 seeds with field and multipole errors (crosses). For the field errors a 0.2% rms variation of all gradients in the dipoles only was assumed. Top: On-energy DA. Bottom: Off-energy DA.

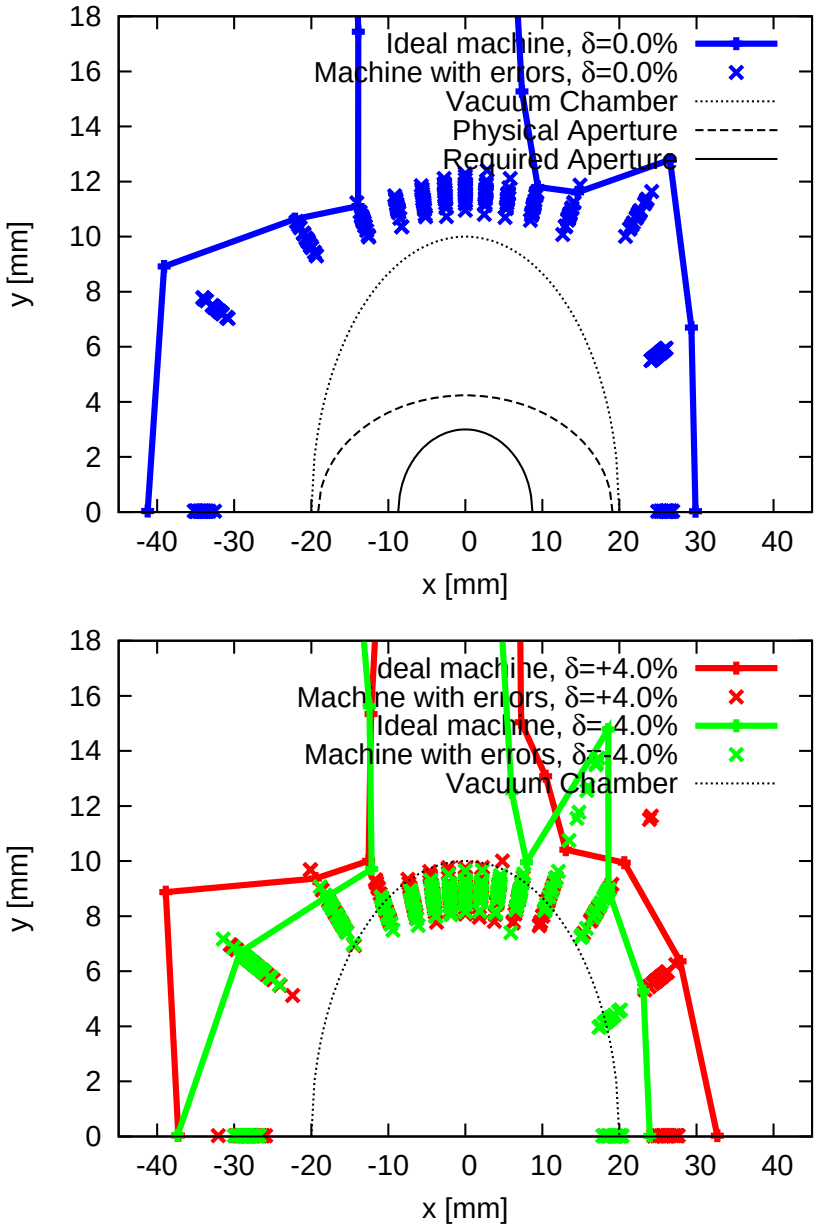

Figure 17: Dynamic aperture at the center of the straight section in the MAX IV 1.5 GeV storage ring (bare lattice) from tracking with Tracy-3. The plots show the ideal lattice (solid line) and results for 20 seeds with field and multipole errors (crosses). For the field errors a 0.02% rms variation of all gradients in the dipoles and quadrupoles as well as a 0.02% rms variation of all sextupole gradients was assumed. Top: On-energy DA. Bottom: Off-energy DA.

4.1.3 The Combined Effect of all Errors

The final step is to generate the DA of a bare lattice when all error models are combined in order to model a machine that comes closest to a realistic machine. This is displayed in Fig. 18. The important conclusion is that if the dipole gradients can be corrected to within 0.02% rms through shunting or individual power supplies, a DA beyond the vacuum aperture should be achievable. This is a highly desirable situation as it guarantees highest injection efficiency as well as lifetime determined solely by the physical apertures which have been designed with target lifetime in mind.

To reaffirm the importance of reducing variations in the dipole gradients, another parameter set has been studied. The overall DA has been assessed for a machine where in addition to the alignment and multipole errors, field errors with 0.2% rms variation of the gradients in all quadrupoles and sextupoles have been assumed. For the dipole gradients however, it is assumed that the variation can be suppressed to 0.02% rms. The results are displayed in Fig. 19. Again, the overall on-momentum DA is more than sufficient. In conclusion, while larger gradient variations in the sextupoles and quadrupoles can be tolerated, the dipole gradients should be corrected carefully in order to restore design DA and consequently highest injection efficiency and good Touschek lifetime.

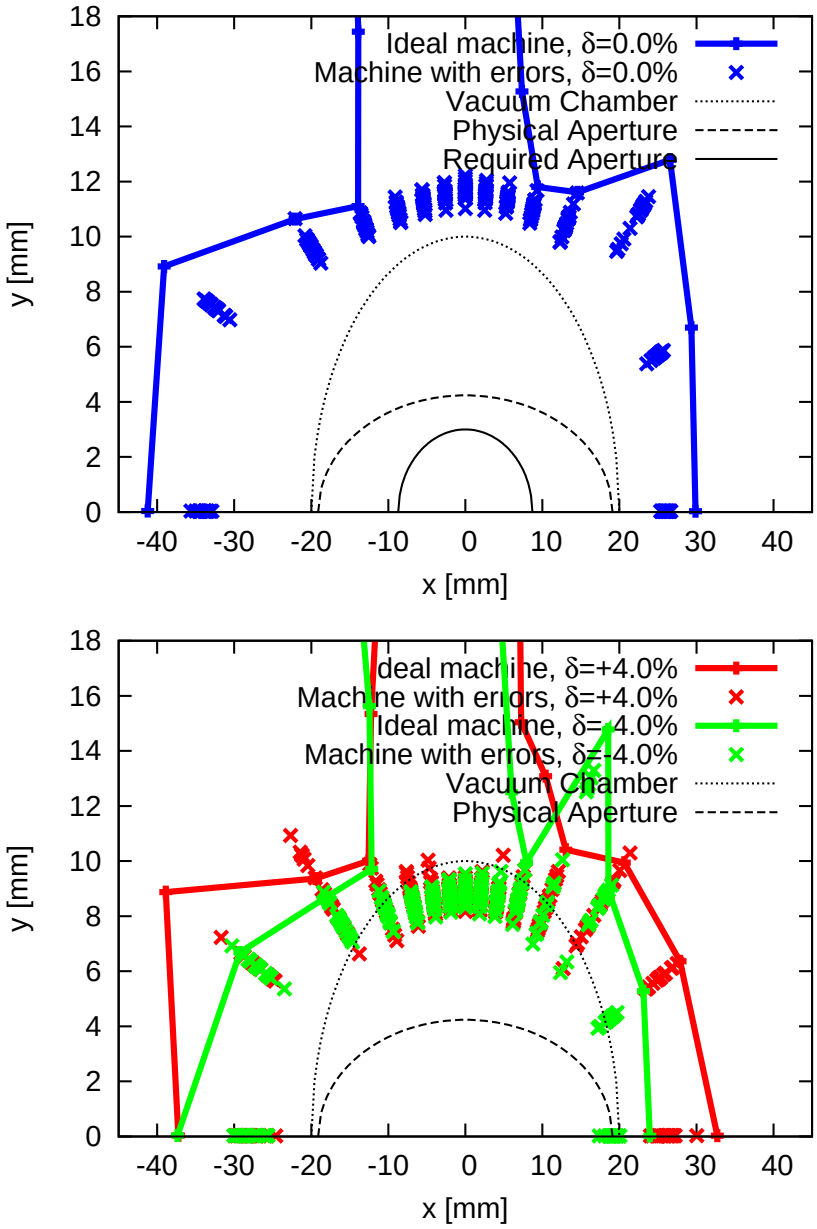

Figure 18: Dynamic aperture at the center of the straight section in the MAX IV 1.5 GeV storage ring (bare lattice) from tracking with Tracy-3. The plots show the ideal lattice (solid line) and results for 20 seeds with misalignments as well as field and multipole errors (crosses). For the field errors a 0.02% rms variation of all gradients in the dipoles and quadrupoles as well as a 0.02% rms variation of all sextupole gradients was assumed. Top: On-energy DA. Bottom: Off-energy DA.

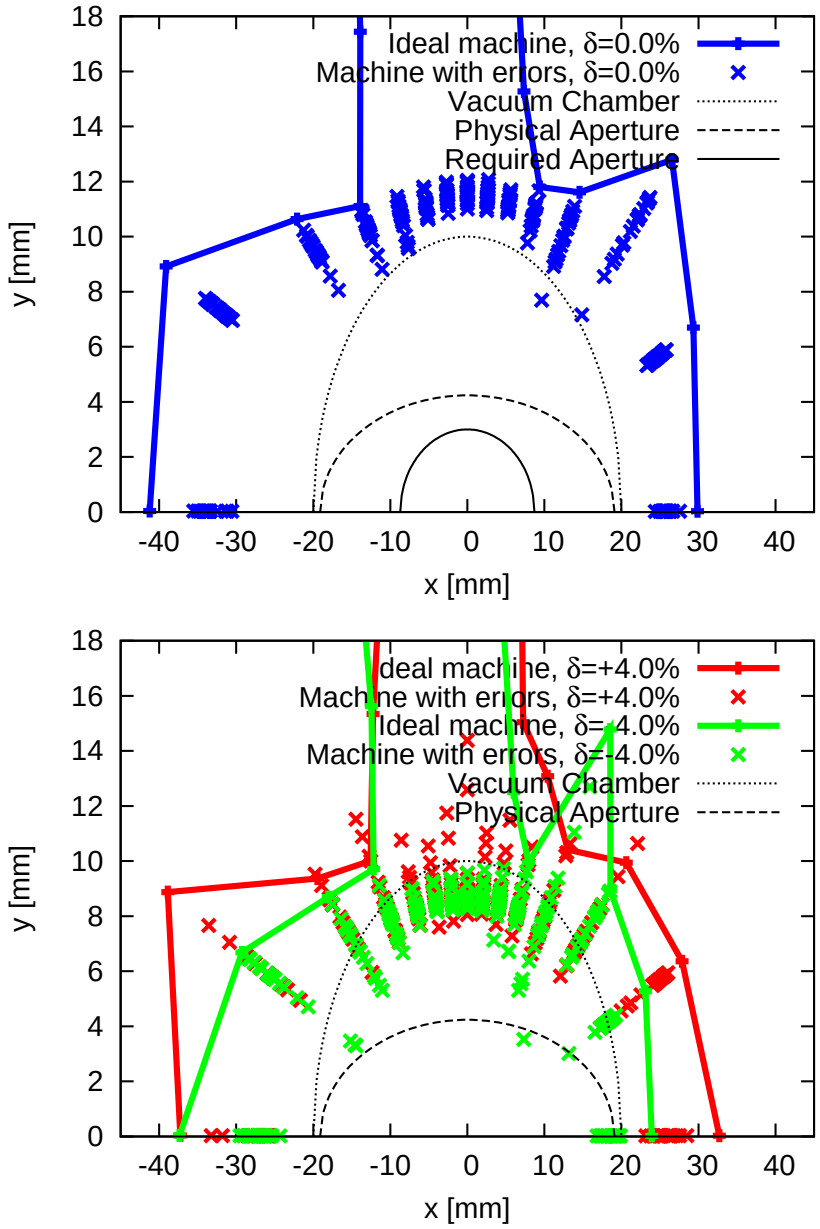

Figure 19: Dynamic aperture at the center of the straight section in the MAX IV 1.5 GeV storage ring (bare lattice) from tracking with Tracy-3. The plots show the ideal lattice (solid line) and results for 20 seeds with misalignments as well as field and multipole errors (crosses). For the field errors a 0.2% rms variation of all quadrupole and sextupole gradients as well as a 0.02% rms variation of all dipole gradients was assumed. Top: On-energy DA. Bottom: Off-energy DA.

4.2 Emittance, Intrabeam Scattering, Touschek Lifetime

4.2.1 Intrabeam Scattering

Because the emittance of the MAX IV 1.5 GeV storage ring lattice is not ultralow, intrabeam scattering (IBS) is not expected to have the significant influence on overall equilibrium emittance that it has for the 3 GeV storage ring. Emittance values given so far take into account the emission of synchrotron radiation and quantum emission fluctuations, but not IBS. In this section, emittance growth from IBS is briefly calculated to verify that IBS can be neglected in the case of the 1.5 GeV storage ring.

IBS calculations have been performed with Tracy-3 using expected rf parameters (cf. DDR Section 3.6.2). The results calculated for a total stored current of 500 mA ($\rightarrow$ bunch charge $Q_b = 5$ nC), expected rf parameters (radiation losses of the bare lattice 114.1 keV/turn, total cavity voltage 560 kV $\rightarrow$ rf acceptance $\sigma_{\rm rf} = 4.127\%$, rms bunch length $\sigma_s = 14.58$ mm), and coupling set to 1% ($\rightarrow \varepsilon_y = 60$ pm rad) are summarized in Table 3. The table compares the values for the bare lattice with those for a bare lattice with harmonic Landau cavities (LC's) running at 300 MHz ($\sigma_s = 14.58$ mm $\rightarrow 60$ mm). As expected, as soon as the LC's are tuned in, IBS can be neglected in the MAX IV 1.5 GeV storage ring.

Table 3: Effect of IBS on the MAX IV 1.5 GeV storage ring. The bare lattice emittance has been calculated assuming coupling adjusted to 1% to give $\varepsilon_y = 60$ pm rad. The influence of the harmonic Landau cavities (LC's) is also shown. Emittance growth and bunch lengthening from IBS become entirely negligible once the LCs are operated.

	ε_x [nm rad]			σ_s [mm]		
MAX IV 1.5 GeV	5.98	$\rightarrow$	6.08	14.58	$\rightarrow$	14.91
MAX IV 1.5 GeV with LC's	5.98	$\rightarrow$	6.01	60.0	$\rightarrow$	60.35

4.2.2 Touschek Lifetime

Since Touschek lifetime depends strongly on charge density in 6D phase space it varies as a function of transverse emittances (including IBS) as well as bunch lengthening from Landau cavities. Because of this nontrivial interplay between several factors in the realistic machine, the plan here will be to investigate several "base line" configurations of the MAX IV 1.5 GeV storage ring and then show consequences

for variation of specific parameters like main cavity voltage or bunch lengthening achieved with the LCs. All calculations shall be carried out assuming 500 mA stored beam current in all buckets with no ion-clearing gap (i.e. 5 nC charge per bunch).

The MAX IV 1.5 GeV storage ring has two main rf cavities for a maximum overall accelerating voltage of 560 kV. The ring also has two third-harmonic LC's that should allow bunch lengthening by up to $\approx$ 70 mm rms (roughly a factor 5!). The lattice was originally designed to give a momentum acceptance (MA) of 4%. Figure 20 shows the MA for one achromat of the bare lattice using standard vacuum chambers:

- 28 mm $\times$ 14 mm (half-apertures) within SQFi and SCi
- 20 mm $\times$ 10 mm (half apertures) within all other magnets and in the straight sections
- aperture restrictions at the septum included

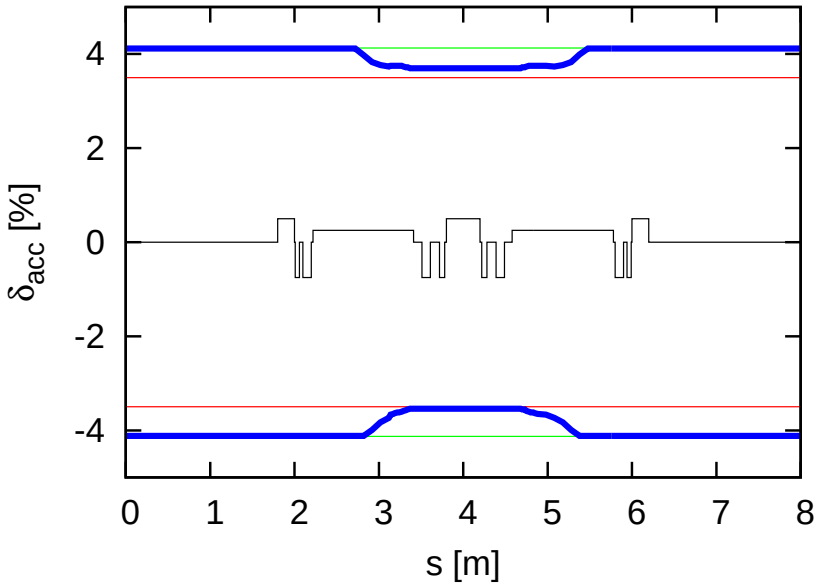

Figure 20: Momentum acceptance for one achromat of the MAX IV 1.5 GeV storage ring. A bare lattice with standard vacuum apertures and cavities at maximum voltage 560 kV have been assumed (green line, corresponds to 4.127% MA). For comparison, the red line shows 3.5% MA (which corresponds to 454 kV in this configuration). The blue line shows overall MA. Tracking was performed with Tracy-3 over one synchrotron period.

Figure 20 assumes that rf cavities are driven at the maximum voltage of 560 kV corresponding to an rf acceptance of 4.127% (green line). The lattice acceptance is indeed around 4%: in most locations it is slightly above, but it is actually a bit lower at the achromatic centers (where peak dispersion values are reached). The resulting overall MA (blue line) is therefore 4% almost everywhere. This holds as long as sufficient rf voltage is available. If the rf voltage is reduced sufficiently it will start to determine the overall MA. This situation is also shown in the figure: if 454 kV overall cavity voltage (red line) is applied, the rf acceptance is reduced to 3.5% (corresponding to the minimum overall MA observed in the nominal case). One consequence of such a situation is that Touschek lifetime calculations in 6D (which are derived from tracking and thus require a lot of CPU time) can be approximated well by a linear simplification (available in both Tracy-3 and OPA) [6].

Table 4 shows results for emittance (including IBS) and Touschek lifetime for the MAX IV 1.5 GeV storage ring bare lattice in different configurations. In all cases the coupling is adjusted to 1% setting the vertical emittance at a diffraction limit of roughly 7.5 Å. At first no LCs are used to stretch the bunches. When IBS is included both emittances increase by the same fraction so the coupling remains 1%. For comparison, the LCs are tuned in to stretch the bunches to 60 mm. If IBS is included this elongates the bunches a bit more, but the overall length is still well within the capabilities of the 3rd harmonic rf system.

Table 4: Overview of emittances, IBS, and Touschek lifetime for different configurations of the bare lattice. Without IBS the natural emittance for this lattice is $\varepsilon_0 = 5.982$ nm rad and the synchrotron radiation losses are 114.1 keV/turn. The total rf voltage has been set to $U_{\mathrm{cav}} = 560$ kV which corresponds to of $\delta_{\mathrm{rf}} = 4.127\%$. The star ($\star$) indicates IBS included. Touschek lifetime figures in parentheses indicates results from linear approximation.

IBS	κ	ε_y [nm rad]	ε_x [pm rad]	σ_s [mm]	$\sigma_\delta \times 10^{-4}$	τ_{ts} [h]
7.5 Å diffraction limit, no LCs						
	1%	5.982	59.82	14.58	7.45	(9.105)
$\star$	1%	6.076	60.757	14.91	7.620	8.538 (9.453)
7.5 Å diffraction limit, LCs tuned in						
	1%	5.982	59.82	60.0	7.45	(37.47)
$\star$	1%	6.006	60.057	60.35	7.493	34.15 (37.83)

The Touschek lifetime (including IBS) is 8.5 h without LCs but 34 h with LCs.

This latter figure is certainly more than sufficient and would actually lead to a situation where the overall lifetime is actually no longer Touschek-dominated (the elastic gas scattering lifetime has been estimated to be 30 h [4]). This is rather unusual for a modern third-generation light source.

As can be inferred from Fig. 20, the overall MA of the bare lattice can be dominated by the rf acceptance if the cavity voltage is set to 454 kV or less. Such a situation is investigated in Table 5. As one would expect, the natural bunch length is increased by the reduced rf acceptance. Since the rf acceptance is now lower than the lattice acceptance throughout the entire machine, the Touschek lifetime calculated with 6D tracking in Tracy-3 is almost identical to the linear approximation from OPA. Touschek lifetime is increased from 6.3 h to 22.6 h by the LCs.

Table 5: Overview of emittances, IBS, and Touschek lifetime for different configurations of the bare lattice. Without IBS the natural emittance for this lattice is $\varepsilon_0 = 5.982$ nm rad and the synchrotron radiation losses are 114.1 keV/turn. The total rf voltage has been set to $U_{\mathrm{cav}} = 454$ kV which corresponds to of $\delta_{\mathrm{rf}} = 3.543\%$. The star ($\star$) indicates IBS included. Touschek lifetime figures in parentheses indicates results from linear approximation.

IBS	κ	ε_y [nm rad]	ε_x [pm rad]	σ_s [mm]	$\sigma_\delta \times 10^{-4}$	τ_{ts} [h]
7.5 Å diffraction limit, no LCs						
	1%	5.982	59.82	16.29	7.45	(6.111)
$\star$	1%	6.066	60.663	16.62	7.603	6.286 (6.325)
7.5 Å diffraction limit, LCs tuned in						
	1%	5.982	59.82	60.0	7.45	(22.51)
$\star$	1%	6.006	60.057	60.35	7.493	22.59 (22.73)

Figure 21 attempts to summarize the bare lattice Touschek lifetime as a function of cavity voltage, i.e. rf acceptance. In the figure the bare lattice has been assumed with 500 mA stored current. The effect of IBS was included, no LCs were assumed, i.e. the natural bunch length with IBS lengthening only was applied. Emittance coupling was again set to 1% so the diffraction limit is at roughly 7.5 Å. At a cavity voltage of around 500 kV the linearized approximation for Touschek lifetime starts to deviate from the actual 6D tracking result. It is here ($\delta_{\mathrm{rf}} \approx 3.8\%$) where the lattice MA starts clipping the rf acceptance. For the cases displayed here the LCs can stretch the bunches by a factor 2–5 which increases Touschek lifetime accordingly.

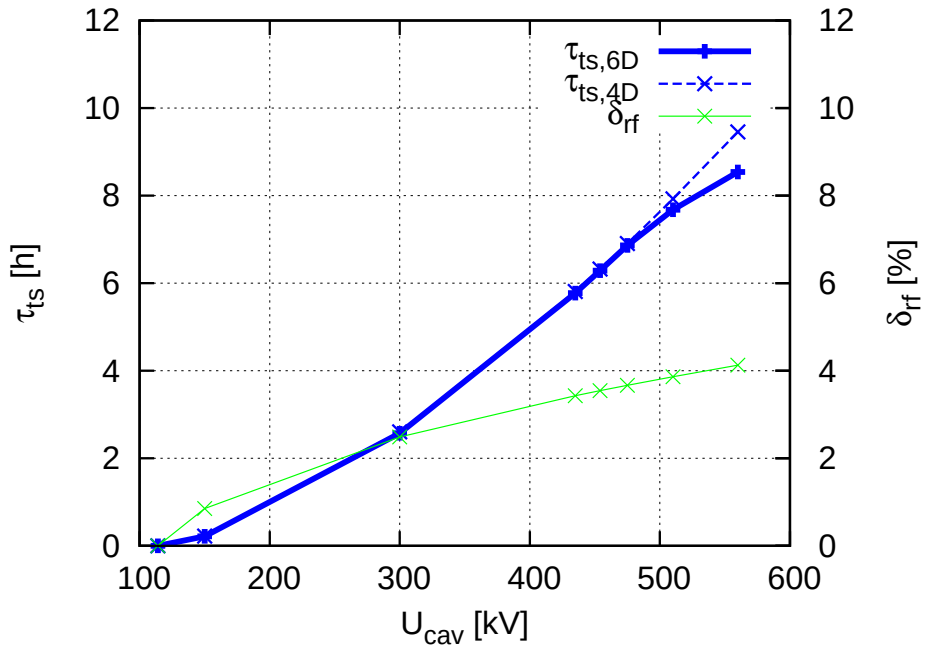

Figure 21: Touschek lifetime (blue) and rf acceptance (green) of the MAX IV 1.5 GeV storage ring bare lattice for different cavity voltages. Standard vacuum chamber apertures and 500 mA stored current were assumed. The effect of IBS was included with coupling set to 1% rendering a diffraction limit at roughly 7.5 Å. No LCs were included.

5 Effect of Insertion Devices

5.1 Optics Matching

As detailed in the DDR, only very strong insertion devices (ID's) will require local and/or global optics matching in the MAX IV 1.5 GeV storage ring. According to current plans, this is mainly an issue for Solaris [7], where at least one superconducting wiggler (SCW) will be installed. This section will therefore study the matching required for the SCW and present the effect this device has on storage ring performance.

Table 6 shows the main parameters of the expected device, a 1.5 m long SCW with 3.5 T maximum field strength. Apart from the increased peak field strength, the device is identical to the device considered in the DDR. In order to prevent beta beating, the local optics (that is, the optics of the DBA on either side of the SCW)

Table 6: Parameters of the 3.5 T SCW.

Length [m]	1.525
Number of periods	25
Period length [mm]	61
Peak magnetic field strength [T]	3.5
Full gap height [mm]	10.2
Radiated energy per turn (at peak strength) [keV]	25.2
Reduction of overall emittance (at peak strength) [nm rad]	0.70

are matched to the device. This requires primarily an increase of vertical focusing, thus reducing the vertical beta function in the SCW to counteract the additional focusing of the ID (which scales with the mean vertical beta function in the ID). This can be performed by changing the vertically focusing gradient in the dipoles flanking the ID (by floating power supplies on the PFS's or by powering these PFS separately from all others). The focusing quadrupoles adjacent to the SCW are also slightly adjusted to match the horizontal beta function and dispersion (maintaining achromaticity). The scaling factors applied to the slices in the model in order to perform this matching are displayed in Table 7.

This local optics matching does leave a residual phase advance (cf. Table 7) that, if left uncorrected, shifts the working point away form its design values. Since the nonlinear dynamics have been carefully tailored to the tune space environment of the design working point, it is desirable to restore the original tunes. This can be carried out by adjusting the horizontal focusing (with the SQFo family) and the vertical focusing (with the PFS's) around the entire ring. Table 8 shows the necessary adjustments and the resulting optics.

Table 7: Adjustments required to match the adjacent achromats to the 3.5 T SCW installed in a straight section of the MAX IV 1.5 GeV storage ring. The relevant change is the increase in vertically focusing gradient strength (+4.5% here) to reduce the vertical beta function within the ID.

Before local adjustment		After local adjustment	
PFS @ SCW: $f_{\mathrm{dip}} = 0.99987651$	$\longrightarrow$	1.04484396	$(+4.5\%)$
SQFo @ SCW: $f_{\mathrm{SQFo}} = 0.98444233$	$\longrightarrow$	0.98495952	$(+0.1\%)$
SQFi @ SCW: $f_{\mathrm{SQFi}} = 0.96939705$	$\longrightarrow$	0.97022787	$(+0.1\%)$
$\Downarrow$		$\Downarrow$	
$\beta_x^* = 5.684\,\mathrm{m}$	$\longrightarrow$	$5.685\,\mathrm{m}$	
$\beta_y^* = 7.074\,\mathrm{m}$	$\longrightarrow$	$2.837\,\mathrm{m}$	
$\eta_x^* \neq 0.0\,\mathrm{m}$	$\longrightarrow$	$0.0\,\mathrm{m}$	
	but also:		
		$\Delta\nu_x = -0.0043$	
		$\Delta\nu_y = +0.1751$	

Table 8: Adjustments required to re-establish the original working point after insertion of the 3.5 T SCW in the MAX IV 1.5 GeV storage ring. The largest change is the compensation of an excess -0.5% vertical phase advance.

Before global adjustment		After global adjustment	
all PFS's: $f_{\mathrm{dip}} = 0.99987651$	$\longrightarrow$	0.99480697	(-0.51%)
all SQFo: $f_{\mathrm{SQFo}} = 0.98444233$	$\longrightarrow$	0.98403231	(-0.04%)
$\Downarrow$		$\Downarrow$	
$\Delta\nu_x = -0.0043$	$\longrightarrow$	$\nu_x = 11.220$	
$\Delta\nu_y = +0.1751$	$\longrightarrow$	$\nu_y = 3.150$	
	leaving:		
		$\beta_x^* = 5.685\,\mathrm{m}$	
		$\beta_y^* = 3.158\,\mathrm{m}$	$(+11.3\%)$
		$\eta_x^* < 0.002\,\mathrm{m}$	

Once this matching has been performed, the linear optics are restored reasonably well. The nonlinear optics are however perturbed slightly by this matching. Without any further adjustment of the sextupoles in the lattice, the chromaticity and the amplitude-dependent tune shift (ADTS) will show slightly different behavior compared to the nominal case for the 523 nonlinear optics. The plots in Figs. 22 and 23 show these deviations.

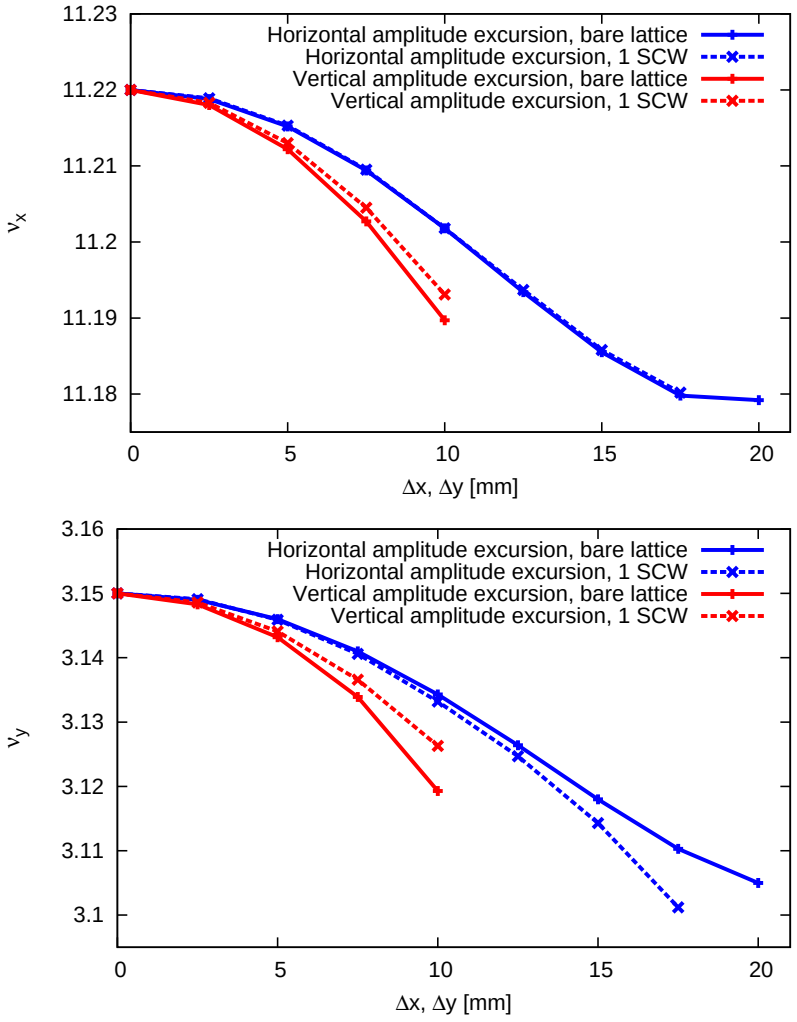

Figure 22: Amplitude-dependent tune shift calculated for the new m5-20120313-523 optics of the MAX IV 1.5 GeV storage ring. The plot compares the bare lattice to the lattice where one SCW has been installed.

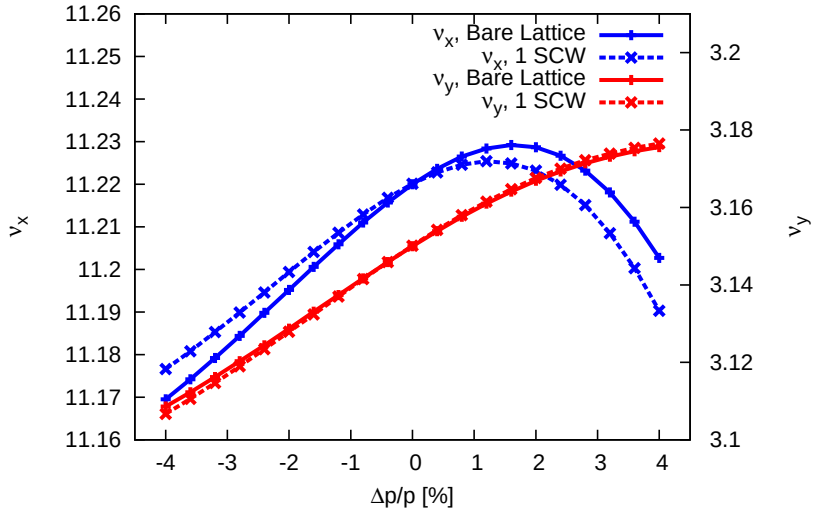

Figure 23: Chromaticity calculated for the new m5-20120313-523 optics of the MAX IV 1.5 GeV storage ring. The plot compares the bare lattice to the lattice where one SCW has been installed.

Since the deviations in the chromaticity and ADTS are small, the tune footprint of the 523 lattice with one SCW but no modification in the sextupole settings (shown in Fig. 24) remains very similar to the original 523 bare lattice footprint (cf. Fig. 6). As a result, also the DA of the 523 lattice with one SCW (cf. Fig. 25) is fairly similar to the bare lattice DA. Since sufficient DA can be achieved without adjusting the nonlinear optics to follow the linear optics matching, it can be concluded that only the linear optics need to be matched to the SCW and that the nonlinear optics can be left at their bare lattice setting. This is a substantial operational advantage.

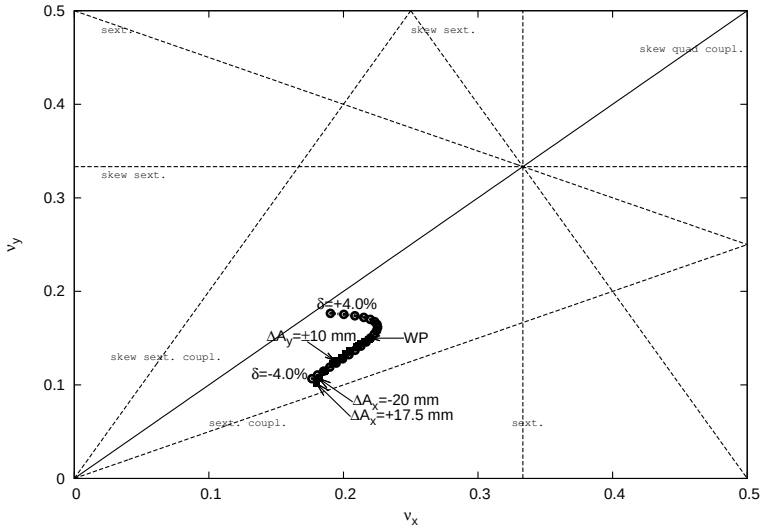

Figure 24: The tune footprint of the new m5-20120313-523 optics of the MAX IV 1.5 GeV storage ring where one SCW has been installed in an otherwise bare lattice.

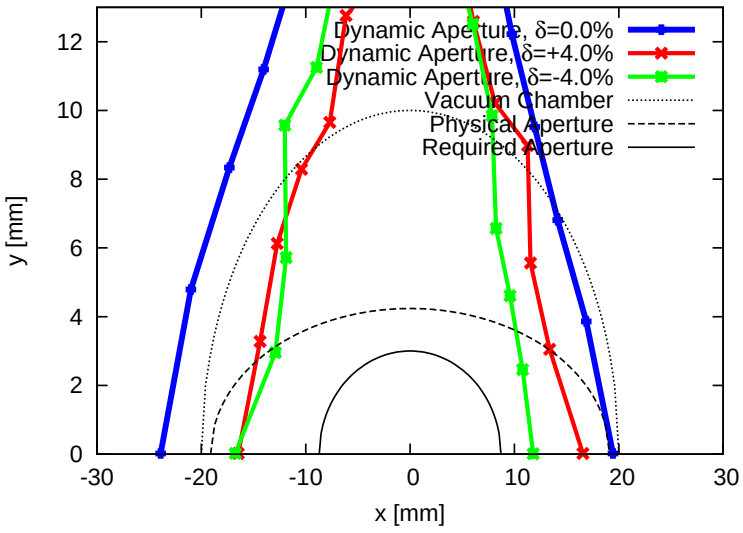

Figure 25: Dynamic aperture calculated with Tracy-3 in 6D for the new m5-20120313-523 optics of the MAX IV 1.5 GeV storage ring where one SCW has been installed in an otherwise bare lattice..

5.2 Effect of Errors

As in Section 4.1.3 for the bare lattice, for a lattice with a single 3.5 T SCW, studies have been performed where all the different errors models have been applied to a lattice. The error models have not been altered. For the field errors it is again assumed that gradients are shunted to an rms variation of 0.2% in all quadrupoles and sextupoles, while the gradient variations in the dipoles are 0.02% rms. The results are displayed in Fig. 26. Even with the SCW, the overall DA is still more than sufficient.

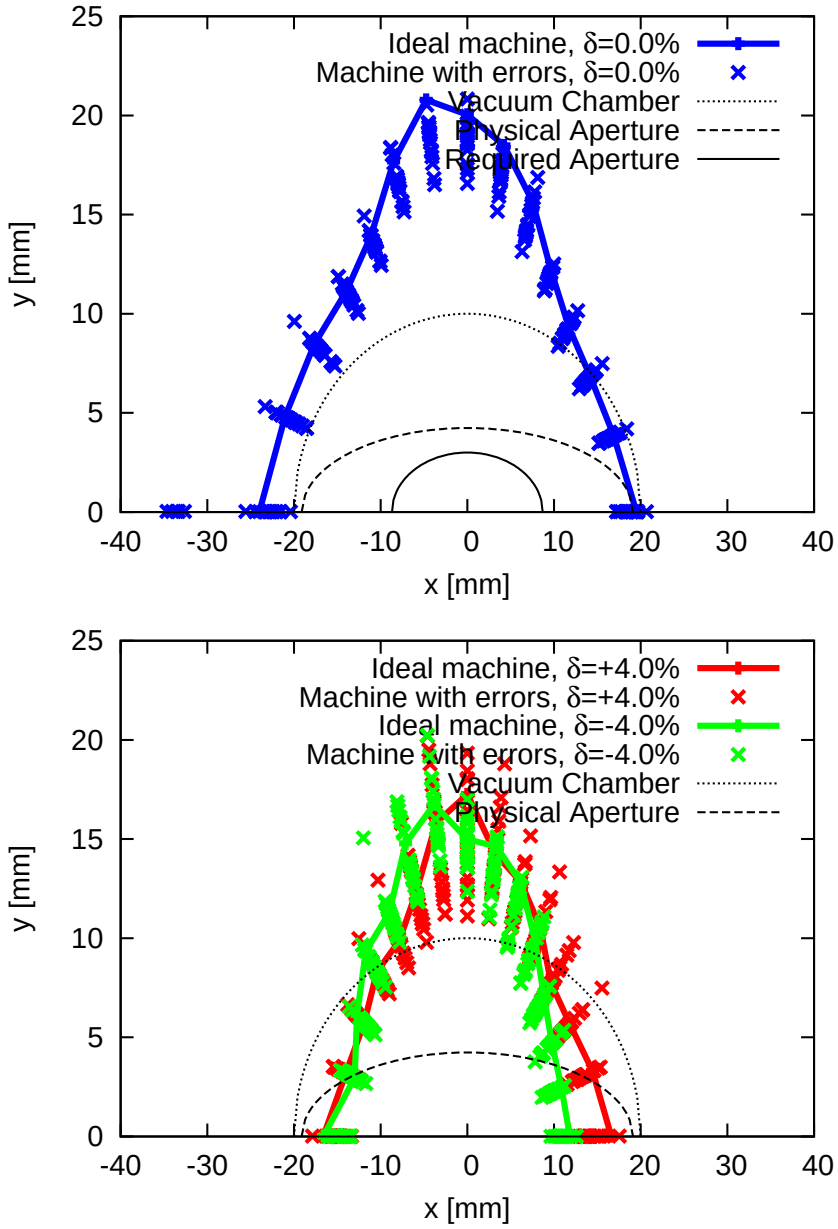

Figure 26: Dynamic aperture at the center of the straight section in the MAX IV 1.5 GeV storage ring (one 3.5 T SCW installed) from tracking with Tracy-3. The plots show the ideal lattice (solid line) and results for 20 seeds with misalignments as well as field and multipole errors (crosses). For the field errors a 0.2% rms variation of all quadrupole and sextupole gradients as well as a 0.02% rms variation of all dipole gradients was assumed. Top: On-energy DA. Bottom: Off-energy DA.

5.3 Effect on Emittance and Lifetime

For the lattice with a single a single 3.5 T SCW emittance, MA, and lifetime need to be revisited. The emittance decrease and increase of radiated power caused by the SCW changes the equilibrium parameters substantially. These changes shall be summarized here and their effect on lifetime will be detailed.

For the lattice with a single 3.5 T SCW, IBS calculations have been performed with Tracy-3 using expected rf parameters (cf. DDR Section 3.6.2). The results calculated for a total stored current of 500 mA ($\rightarrow$ bunch charge $Q_b = 5$ nC), expected rf parameters (radiation losses of the bare lattice 139.3 keV, total cavity voltage 560 kV $\rightarrow$ rf acceptance $\sigma_{\rm rf} = 3.949\%$, rms bunch length $\sigma_s = 15.82$ mm), and coupling set to 1% ($\rightarrow \varepsilon_y = 60$ pm rad) are summarized in Table 9. The table compares the values for the natural bunch length with those for a situation where the harmonic Landau cavities (LC's) at 300 MHz have been tuned in ($\sigma_s = 15.82$ mm $\rightarrow 60$ mm). As already seen in the bare lattice case (cf. Section 4.2.1), as soon as the LC's are tuned in, IBS can be neglected in the MAX IV 1.5 GeV storage ring.

Table 9: Effect of IBS on the MAX IV 1.5 GeV storage ring when one 3.5 T SCW has been installed. For comparison, the bare lattice results from Table 3 have been included. The lattice emittance has been calculated assuming coupling adjusted to 1% to give $\varepsilon_y = 60$ pm rad. The influence of the harmonic Landau cavities (LC's) is also shown. Emittance growth and bunch lengthening from IBS become entirely negligible once the LCs are operated.

	ε_x [nm rad]			σ_s [mm]		
MAX IV 1.5 GeV, bare lattice	5.98	$\rightarrow$	6.08	14.58	$\rightarrow$	14.91
MAX IV 1.5 GeV, one SCW	5.23	$\rightarrow$	5.31	15.82	$\rightarrow$	16.08
MAX IV 1.5 GeV, bare lattice, with LC's	5.98	$\rightarrow$	6.01	60.0	$\rightarrow$	60.35
MAX IV 1.5 GeV, one SCW, with LC's	5.23	$\rightarrow$	5.25	60.0	$\rightarrow$	60.27

Since the added radiated power from the SCW reduces the rf acceptance, the overall MA is also reduced. Minimum levels at the DBA centers now reach about 3% (cf. Fig. 27).

Table 10 shows results for emittance (including IBS) and Touschek lifetime for the MAX IV 1.5 GeV storage ring lattice with one 3.5 T SCW in different configurations. In all cases the coupling is adjusted to 1% setting the vertical emittance at a diffraction limit of roughly 7.5 Å. At first no LCs are used to stretch the bunches.

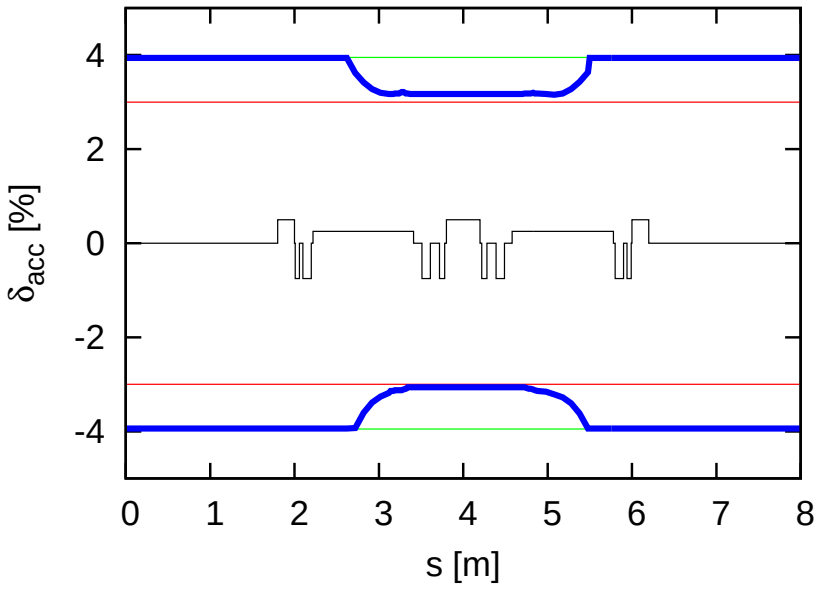

Figure 27: Momentum acceptance for one achromat of the MAX IV 1.5 GeV storage ring. A lattice with one 3.5 T SCW, standard vacuum apertures and cavities at maximum voltage 560 kV have been assumed (green line, corresponds to 3.949% MA). For comparison, the red line shows 3% MA (which corresponds to 402 kV in this configuration). The blue line shows overall MA. Tracking was performed with Tracy-3 over one synchrotron period.

When IBS is included both emittances increase by the same fraction so the coupling remains 1%. For comparison, the LCs are tuned in to stretch the bunches to 60 mm. If IBS is included this elongates the bunches a bit more, but the overall length is still well within the capabilities of the 3rd harmonic rf system.

The Touschek lifetime (including IBS) is 6.4 h without LCs but 24 h with LCs. This latter figure is certainly more than sufficient and would actually lead to a situation where the overall lifetime is just barely Touschek-dominated (the elastic gas scattering lifetime has been estimated to be 30 h [4]).

Table 10: Overview of emittances, IBS, and Touschek lifetime for different configurations of a lattice with one 3.5 T SCW. Without IBS the natural emittance for this lattice is $\varepsilon_0 = 5.228\,\text{nm rad}$ and the synchrotron radiation losses are 139.3 keV/turn. The total rf voltage has been set to $U_{\text{cav}} = 560\,\text{kV}$ which corresponds to of $\delta_{\text{rf}} = 3.949\%$. The star ($\star$) indicates IBS included. Touschek lifetime figures in parentheses indicates results from linear approximation.

IBS	κ	ε_y [nm rad]	ε_x [pm rad]	σ_s [mm]	$\sigma_\delta \times 10^{-4}$	τ_{ts} [h]
7.5 Å diffraction limit, no LCs						
	1%	5.228	52.28	15.82	8.05	(7.921)
$\star$	1%	5.311	53.11	16.08	8.181	6.400 (8.164)
7.5 Å diffraction limit, LCs tuned in						
	1%	5.228	52.28	60.0	8.05	(30.04)
$\star$	1%	5.251	52.51	60.27	8.086	23.72 (30.30)

6 Current Lattice Files

Table 11 lists all current lattice files [3] and what type of elements are included. The lattice files are human-readable and in Tracy-3 format. All lattice files contain BPM's and correctors (SOFB). Girder markers are also included.

Table 11: List of all current lattice files.

File name	Lattice contains
m5-20120313-521-bare.lat	Bare lattice, injection elements included, chromaticity corrected to +2.0 in iron
m5-20120313-523-bare.lat	Bare lattice, injection elements included, chromaticity corrected to +1.0 with SCi/o

References

[1] M. Johansson, draft of an updated DDR Chapter 3.5, unpublished, March 8, 2012.

[2] J. Ahlbäck, private communication, March 2012.

[3] The updated lattice files can be found at `http://www.maxlab.lu.se/node/999`

[4] The MAX IV Detailed Design Report, available at `http://www.maxlab.lu.se/node/1136`

[5] L.J. Lindgren, draft of an updated DDR Chapter 3.7, unpublished, November 8, 2011.

[6] A. Streun, Momentum acceptance and Touschek lifetime, SLS Internal Note 18/97, `http://ados.web.psi.ch/slsnotes/sls1897a.pdf`.

[7] C. Bocchetta et al., "Project Status of the Polish Synchrotron Radiation Facility Solaris", Proceedings of IPAC'11, San Sebastían, Spain, 2011, THPC054, p. 3014.